

# Titanite composition and SHRIMP U–Pb dating as indicators of post-magmatic tectono-thermal activity: Variscan I-type tonalites to granodiorites, the Western Carpathians

PAVEL UHER<sup>1,✉</sup>, IGOR BROSKA<sup>2</sup>, EWA KRZEMIŃSKA<sup>3</sup>, MARTIN ONDREJKA<sup>1</sup>, TOMÁŠ MIKUŠ<sup>4</sup> and TOMÁŠ VACULOVIČ<sup>5</sup>

<sup>1</sup>Department of Mineralogy and Petrology, Faculty of Natural Sciences, Comenius University, Ilkovičova 6, 842 15 Bratislava, Slovakia; ✉pavel.uher@uniba.sk

<sup>2</sup>Earth Science Institute, Slovak Academy of Sciences, Dúbravská cesta 9, 840 05 Bratislava, Slovakia

<sup>3</sup>Polish Geological Institute – National Research Institute, Rakowiecka Street 4, 00-975 Warszawa, Poland

<sup>4</sup>Earth Science Institute, Slovak Academy of Sciences, Banská Bystrica branch, Dumbierska 1, 974 01 Banská Bystrica, Slovakia

<sup>5</sup>Department of Chemistry, Faculty of Science, Masaryk University, Kamenice 5, 625 00 Brno, Czech Republic

(Manuscript received December 3, 2018; accepted in revised form November 11, 2019)

**Abstract:** Titanite belongs to the common accessory minerals in Variscan (~360–350 Ma) metaluminous to slightly peraluminous tonalites to granodiorites of I-type affinity in the Tatric and Veporic Units, the Western Carpathians, Slovakia. It forms brown tabular prismatic-dipyramidal crystals (~0.5 to 10 mm in size) in association with quartz, plagioclase, and biotite. Titanite crystals commonly shows oscillatory, sector and convolute irregular zonal textures, reflecting mainly variations in Ca and Ti versus Al (1–2 wt. % Al<sub>2</sub>O<sub>3</sub>, 0.04–0.08 Al *apfu*), Fe (0.6–1.6 wt. % Fe<sub>2</sub>O<sub>3</sub>, 0.02–0.04 Fe *apfu*), REE (La to Lu+Y; ≤4.8 wt. % REE<sub>2</sub>O<sub>3</sub>, ≤0.06 REE *apfu*), and Nb (up to 0.5 wt. % Nb<sub>2</sub>O<sub>5</sub>, ≤0.01 Nb *apfu*). Fluorine content is up to 0.5 wt. % (0.06 F *apfu*). The compositional variations indicate the following principal substitutions in titanite: REE<sup>3+</sup>+Fe<sup>3+</sup>=Ca<sup>2+</sup>+Ti<sup>4+</sup>, 2REE<sup>3+</sup>+Fe<sup>2+</sup>=2Ca<sup>2+</sup>+Ti<sup>4+</sup>, and (Al,Fe)<sup>3+</sup>+(OH,F)=Ti<sup>4+</sup>+O<sup>2-</sup>. The U–Pb SHRIMP dating of titanite reveal their Variscan ages in an interval of 351.0±6.5 to 337.9±6.1 Ma (Tournaisian to Visean); titanite U–Pb ages are thus ~5 to 19 Ma younger than the primary magmatic zircon of the host rocks. The Zr-in-titanite thermometry indicates a relatively high temperature range of titanite precipitation (~650–750 °C), calculated for assumed pressures of 0.2 to 0.4 GPa and *a*(TiO<sub>2</sub>)=0.6–1.0. Consequently, the textural, geochronological and compositional data indicate relatively high-temperature, most probably early post-magmatic (subsidius) precipitation of titanite. Such titanite origin could be connected with a subsequent Variscan tectono-thermal event (~340±10 Ma), probably related with younger small granite intrusions and/or increased fluid activity. Moreover, some titanite crystals show partial alteration and formation of secondary titanite (depleted in Fe and REE)+allanite-(Ce) veinlets (Sihla tonalite, Veporic Unit), which probably reflects younger Alpine (Cretaceous) tectono-thermal overprint of the Variscan basement of the Western Carpathians.

**Keywords:** titanite, I-type granites, Zr-in-titanite thermometry, LA-ICP-MS analyses, SHRIMP U–Pb dating, Western Carpathians.

## Introduction

Titanite [previously sphene, CaTi(SiO<sub>4</sub>)O] together with rutile and ilmenite belongs to the most widespread titanium minerals of the Earth. There is a large variability of titanite presence in various lithologies from early Archean to recent, including (ultra)basic, intermediate, acid and alkaline magmatic suites including pegmatites, low-grade to UHP metamorphic rocks, as well as in some hydrothermal and sedimentary environments (e.g., Paul et al. 1981; Bernau & Franz 1987; Nakada 1991; Gieré 1992; Russell et al. 1994; Černý et al. 1995; Bea 1996; Carswell et al. 1996; Bouch et al. 1997; Uher et al. 1998; Castelli & Rubatto 2002; Chakhmouradian et al. 2003; Broska et al. 2007; Cempírek et al. 2008; Xie et al. 2010; Gao

et al. 2011; McLeod et al. 2011; Chen et al. 2016). The titanite structure (Speer & Gibbs 1976; Liferovich & Mitchell 2005, 2006) comprises three different cation sites plus five anion sites, and the general formula of the titanite-group minerals can be written as XYZO<sub>4</sub>W. The sites are inhabited by following cations: the tetrahedral Z site hosts Si<sup>4+</sup> (and possibly small amounts of Al<sup>3+</sup>, Ti<sup>4+</sup>, P<sup>5+</sup>, As<sup>5+</sup>, S<sup>6+</sup>, and vacancy), the octahedral Y site occupies Ti<sup>4+</sup> and various small to medium-sized cations (Mg<sup>2+</sup>, Fe<sup>2+</sup>, Fe<sup>3+</sup>, Al<sup>3+</sup>, Sc<sup>3+</sup>, Cr<sup>3+</sup>, Mn<sup>3+</sup>, As<sup>3+</sup>, Sb<sup>3+</sup>, V<sup>3+</sup>, V<sup>4+</sup>, Sn<sup>4+</sup>, Zr<sup>4+</sup>, Hf<sup>4+</sup>, Si<sup>4+</sup>, V<sup>5+</sup>, Nb<sup>5+</sup>, Ta<sup>5+</sup>, As<sup>5+</sup>, Sb<sup>5+</sup>, W<sup>6+</sup>), the 7-coordinated X site polyhedra contain Ca<sup>2+</sup> and other mainly medium- to large-sized cations: Na<sup>+</sup>, K<sup>+</sup>, Fe<sup>2+</sup>, Mn<sup>2+</sup>, Sr<sup>2+</sup>, Ba<sup>2+</sup>, Pb<sup>2+</sup>, REE<sup>3+</sup> (La<sup>3+</sup> to Lu<sup>3+</sup> and Y<sup>3+</sup>), Th<sup>4+</sup>, and U<sup>4+</sup>, whereas the anionic W site is occupied dominantly by O<sup>2-</sup>,

(OH)<sup>-</sup>, F<sup>-</sup>, and Cl<sup>-</sup> (e.g., Ribbe 1980; Bernau & Franz 1987; Gieré 1992; Russel et al. 1994; Černý et al. 1995; Perseil & Smith 1995; Knoche et al. 1998; Brugger & Gieré 1999; Della Ventura & Bellatreccia 1999; Markl & Piazzolo 1999; Chakhmouradian 2004; Cempírek et al. 2008; Xie et al. 2010; Stepanov et al. 2012; Pieczka et al. 2017).

The wide compositional variability of titanite reflects different conditions of the host-rock formation and the mineral is widely used in genetic interpretations. Especially, the content of Zr in titanite, proportional to temperature and pressure of its precipitation, is successfully used in the application of the Zr-in-titanite thermobarometer (Hayden et al. 2008). Moreover, admixtures of radioactive actinides (U and Th isotopes) and their decay products (Pb isotopes) in titanite structure enable to measure the radiometric age of titanite formation (e.g., Burger et al. 1965; Tilton & Grunefelder 1968; Resor et al. 1996; Kennedy et al. 2010; Sun et al. 2012; Gasser et al. 2015; Kohn 2017), recently also combined with oxygen isotope distribution across titanite crystals (Bonamici et al. 2015). Consequently, titanite composition and isotope characteristics represent valuable tools for the understanding of the host-rock origin and tracers of various geological processes, widely used by petrochronology as well as P–T–t path reconstructions (e.g., Rubatto & Hermann 2001; Castelli & Rubatto 2002; Gao et al. 2011; Kohn & Corrie 2011; Stearns et al. 2015; Kirkland et al. 2016, 2018; Kohn 2017).

Titanite is a characteristic accessory mineral of granitic rocks, from metaluminous to slightly peraluminous biotite-±hornblende-bearing tonalites and granodiorites of calc-alkaline, orogenic-related suites (e.g., Lyakhovich 1968; Wones 1989; Bea 1996; Hoskin et al. 2000; McLeod et al. 2011). Titanite is also a typical accessory mineral in Variscan granitic rocks of I-type affinity in the Western Carpathians, Slovakia (e.g., Schafarzík 1898; Radziszewski 1924; Hovorka 1960; Hovorka & Hvožd'ara 1964; Jacko & Petrik 1987; Broska & Uher 1988; Petrik & Broska 1989, 1994; Broska et al. 1997). Recently, the West-Carpathian granitic titanite has been investigated in detail, including its electron-microprobe chemical composition, <sup>57</sup>Fe Mössbauer spectroscopy, associated minerals, and alteration products (Broska et al. 2004, 2007; Broska & Petrik 2015).

Despite above-mentioned results, some aspects of titanite chemical composition are still not resolved. Moreover, age and origin of titanite from the West-Carpathian Variscan granitic rocks have been interpreted controversially: as a product of Alpine (Cretaceous) post-magmatic, syn- to post-tectonic recrystallization of parental granodiorite/tonalite (Zoubek 1936) or as a result of Variscan (Carboniferous) primary magmatic (Hovorka 1960; Hovorka & Hvožd'ara 1964) to late-magmatic precipitation (Broska et al. 2004, 2007). This paper presents a detailed study of titanite in the Variscan I-type granites of the Western Carpathians, including their compositional variations (main and trace element chemistry) with main substitution mechanisms, as well as in-situ U–Pb dating and possible genetic scenario based on titanite thermobarometry and chronometry. Such research is a contribution to

our understanding of titanite origin and evolution of the host granitic rocks.

## Regional geology

The Western Carpathians form a part of the Alpine orogenic belt, divided into the Inner and Outer Western Carpathians (Bezák et al. 2011). The Paleozoic basement rocks of the Inner Western Carpathians occur in three Alpine tectonic units: Tatric, Veporic, and Gemic. The Variscan (Devonian to Carboniferous) calc-alkaline granitic plutons of I- and S-type affinity (e.g., Petrik & Kohút 1997; Kohút et al. 1999; Broska & Uher 2001; Kohút & Nabelek 2008; Broska et al. 2013) occur in the Tatric and Veporic units, they intruded high- to medium-grade Paleozoic metamorphic rocks (mainly metapelites to metapsammities) of the Variscan nappes, which show a pre-Alpine, generally south vergency (e.g., Putiš 1992; Bezák et al. 1997; Bielik et al. 2004). Moreover, small bodies of Permian post-orogenic to anorogenic S- and A-type granitic rocks are also present in various tectonic units of the Inner Western Carpathians, mainly in the Gemic Unit (e.g., Uher & Broska 1996; Broska & Uher 2001).

The West-Carpathian Variscan I-type granitic rocks are represented by coarse- to medium-grained, usually equigranular to slightly porphyric, biotite, locally hornblende-bearing (leuco)tonalites to granodiorites, rarely more evolved two-mica granites. Fluorapatite, zircon, allanite-(Ce), epidote, magnetite, pyrite and titanite belong to widespread accessory mineral of these granitic rocks. Moreover, the tonalites to granodiorites sporadically contain small bodies of mafic microgranular enclaves of diorite to melatonalite composition (Petrik & Broska 1989) and rare dykes of granitic pegmatites (Uher & Broska 1995). In contrast to the undeformed I-type granitic rocks of the Tatric Unit, those of the Veporic Unit commonly show Paleo-Alpine (Cretaceous) metamorphic overprint manifested by mildly to strong post-magmatic alteration of primary magmatic minerals, especially plagioclase, biotite and allanite-(Ce).

These granitic rocks reveal calc-alkaline, metaluminous to the slightly peraluminous character with slightly elevated contents of Ca, Mg, Sr, Ba, Ti, Zr and P, and low K, Rb, Li, B, Sn and F concentrations (Broska & Uher 2001). The whole-rock REE patterns are relatively steep ( $La_N/Lu_N=10-40$ ), usually with slightly negative Eu anomaly ( $Eu_N/Eu_N^*=0.7-0.9$ ). The chemical composition, Sr and Nd isotopes ( $I_{Sr}=0.705\pm 0.001$ ,  $\epsilon Nd_{350}=-0.6$  to  $-4$ ) suggest subduction-related, I-type character of these granitic rocks, originated by mixing of a deeper-seated mafic melt with mantle signature into the felsic crustal magmatic reservoir (Kohút et al. 1999; Poller et al. 2001; Broska & Petrik 2011; Broska et al. 2013). The zircon in-situ U–Pb isotope dating indicates an Upper Devonian to Lower Carboniferous (Mississippian) crystallization age interval ( $\sim 350$  to  $370$  Ma) for the I-type granitic suite in the Western Carpathians (e.g., Kohút et al. 2009; Broska et al. 2013; Gawęda et al. 2016).

## Methods

Accessory titanite and their host rocks were studied in polished thin sections under a polarizing optical microscope. Moreover, separates of titanite and other accessory minerals were obtained by common procedure: crushing of ~15 kg rock sample, sieving ( $\leq 0.5$  mm size was used) and then by using the Wilfley vibrating table, heavy liquids (bromofrom, methylene iodide) and finally by the Cook electromagnetic separator. Titanite crystals were concentrated mainly in the slightly paramagnetic fraction of heavy mineral separates. Larger titanite crystals (~3–10 mm) were manually separated from the host rock (Sih-1 sample). These separated titanite crystals were fixed and polished in sections of 2.54 cm diameter.

The in situ chemical composition of titanite was analyzed by the JEOL JXA 8530FE electron-probe microanalyser (EPMA) at the Earth Sciences Institute of the Slovak Academy of Sciences in Banská Bystrica at the following conditions: WDS mode, accelerating voltage 15 kV, probe current 20 nA, beam diameter 3  $\mu\text{m}$ , counting time 10–30 s on peak, 5–15 s on background, the ZAF correction. The X-ray lines and used standards are following: Nb ( $L\alpha$ ,  $\text{LiNbO}_3$ ), Si ( $K\alpha$ , albite), Ti ( $K\alpha$ , rutile), Al ( $K\alpha$ , albite), Y ( $L\alpha$ ,  $\text{YPO}_4$ ), La ( $L\alpha$ ,  $\text{LaPO}_4$ ), Ce ( $L\alpha$ ,  $\text{CePO}_4$ ), Pr ( $L\beta$ ,  $\text{PrPO}_4$ ), Nd ( $L\alpha$ ,  $\text{NdPO}_4$ ), Sm ( $L\beta$ ,  $\text{SmPO}_4$ ), Gd ( $L\beta$ ,  $\text{GdPO}_4$ ), Fe ( $K\alpha$ , hematite), Mn ( $K\alpha$ , rhodnite), Mg ( $K\alpha$ , diopside), Ca ( $K\alpha$ , diopside), Na ( $K\alpha$ , albite), K ( $K\alpha$ , orthoclase), and F ( $K\alpha$ , fluorite). The chemical compositional zoning of titanite crystals was studied using the back-scattered electron imaging (BSE) by the EPMA.

The content of trace elements was measured using a Laser Ablation–Inductively Coupled Plasma–Mass Spectrometry (LA–ICP–MS) at the Department of Chemistry, Masaryk University, Brno, which consists of a laser ablation system UP 213 (New Wave Research, Inc., Fremont, U.S.A.) and an ICP–MS spectrometer Agilent 7500 CE (Agilent Technologies, Santa Clara, U.S.A.). The laser-ablation system is equipped with a programmable XYZ-stage to move the sample along a programmed trajectory during ablation. Visual target inspection, as well as the photographic documentation, is accomplished using a built-in microscope/CCD-camera system. The ablation cell was flushed with helium (carrier gas), which transported the laser-induced aerosol to the inductively coupled argon plasma (1 l.min<sup>-1</sup>). A sample gas flow of argon was admixed to helium carrier gas flow after the laser ablation cell. Therefore, the total gas flow was 1.6 l.min<sup>-1</sup>. Laser ablation was performed with a laser spot diameter of 40  $\mu\text{m}$ , laser pulse fluence of 7 J.cm<sup>-2</sup>, and 10 Hz repetition rate for 60 seconds each. The Si was used as an internal standard and the NIST SRM 610 silicate glass calibration standard was applied.

The U–Th–Pb isotope composition used for dating of titanite was analysed by SIMS using the Sensitive High Resolution Ion Microprobe (SHRIMP) technique by the SHRIMP IIe/MC at the Polish Geological Institute – National Research Institute (PGI–NRI), Warszawa. The fragments of selected titanite crystals were mounted on adhesive tape together with chips of

reference Khan titanite (e.g., Heaman 2009) and embedded by epoxy resin (Struers Epofix). After that, the epoxy disc was polished to reveal cross-sections through the grains, cleaned and dried. Finally, the polished titanite crystals were imaged on the Nikon Eclipse LV100NPol optical microscope in transmitted and reflected light mode using the NIS-Elements BR software and on HITACHI SU3500 EPMA using a back-scattered (BSE) detector to check the homogeneity of titanite fragments and to select proper domains for analyses without the presence of different mineral inclusions. The sample mount was then cleaned and coated with gold to yield a conductivity resistance of 10–20  $\Omega$  for the SHRIMP analysis. The basic analytical procedure for titanite on SHRIMP instrument described by Sato et al. (2016) has been slightly modified. The run table for titanite included 6 mass scans of the following 10 peaks: <sup>204</sup>Pb (a background measured at 0.045 mass units above the <sup>204</sup>Pb peak), <sup>200</sup>TiCa<sub>2</sub>O<sub>4</sub> (guide peak), <sup>206</sup>Pb, <sup>207</sup>Pb, <sup>208</sup>Pb, <sup>238</sup>U, <sup>232</sup>Th, ThO, UO, and UO<sub>2</sub>.

The primary ion beam was rastered over a 25–30  $\mu\text{m}$  rectangle for 2.0 minutes prior to each single spot collection, to reduce a surface contributions by common Pb. After that each measurement has six cycles through the data acquisition of 10 peaks, but a total analytical time for one spot is not extended 18 min. The focusing of an O<sup>2-</sup> primary ion beam on sectioned titanite grains typically produces a spot with an elliptical size of about 20–23  $\mu\text{m}$  and depth of 3–4  $\mu\text{m}$ .

The Khan titanite was used as the principal reference material for Pb\*/U and Th\*/Pb. The counts were acquired on both the sample and titanite standard along whole analytical session. The uranium content of 584±95 ppm, according to ID–TIMS characteristics provided by Heaman (2009), and <sup>206</sup>Pb/<sup>238</sup>U age of 518±2 Ma (Kinny et al. 1994) were taken as reference values. During about 24 hours of the analytical session on SHRIMP, twenty Khan analyses yielded a weight average <sup>207</sup>Pb/<sup>206</sup>Pb age of 518±13 Ma (MSWD=1.4) and weight average <sup>238</sup>U/<sup>206</sup>Pb age of 516.6±7.0 Ma (MSWD=1.4). These data set (n=20) gave a lower intercept of age of 517±7 Ma (MSWD=0.96) on the W concordia plot (the diagram not shown). All these calculated Khan datings are within uncertainty of its reference value, showing similarity to other results determined for the Khan titanite by the LA–ICP–MS, ID–TIMS or SHRIMP methods (Kinny et al. 1994; Simonetti et al. 2006; Heaman 2009; Chew et al. 2014; Sato et al. 2016; Ma et al. 2019).

The SQUID2.50.11.01.03 software (Ludwig 2009) and attached the Isoplot/Ex version 3.00 Macro program (Ludwig 2003) were used for data processing. The SQUID2 calculates a ‘calibration constant’, for each analysis of the reference material (RM) and an error-weighted mean and standard error for all of these analyses, plus the error on the calibration, and the external error from the standard dataset. For each analysis of an unknown, a value for blank and its uncertainty is calculated. The ratio <sup>204</sup>Pb\*/<sup>206</sup>Pb, and the estimated <sup>207</sup>Pb\*/<sup>206</sup>Pb age of the titanite, are used to correct for a common Pb composition calculated from the Stacey and Kramers (1975) model of bulk-crustal Pb isotope composition. The spot values for

U–Th–Pb Special equations (Ludwig 2009) were calculated as spot average, and for other Task equations as spot average. The  $^{207}\text{Pb}$  correction for  $^{206}\text{Pb}/^{238}\text{U}$  as Squid option was applied, which assumes concordance between radiogenic  $^{206}\text{Pb}/^{238}\text{U}$  and  $^{207}\text{Pb}/^{235}\text{U}$ . Possibility of this assumption was evaluated by calculation of single analytical session using the concordia age function of SQUID2 software (Ludwig 2009), which has the advantage of providing a test of concordance. Both type of the concordia diagrams of Tera–Wasserburg (T–W) and Wetherill (W) were generated, and values with lower the mean square weighted deviation (MSWD) were preferred. Uncertainties on individual analyses in the data table are reported at a  $1\sigma$  level but calculated on concordia diagrams are reported as a  $2\sigma$ . The error in standard calibration was 0.81 %.

## Results

### Petrography of granitic rocks

We chose six typical samples of titanite-bearing I-type tonalites to granodiorites, located in the Tribeč, Nízke Tatry, Vepor and Čierna Hora Mountains (Fig. 1; see the Appendix for detailed locations). The investigated titanite-bearing granitic rocks are medium- to coarse-grained, biotite tonalites to granodiorites with hypidiomorphic granular texture. Rock-forming minerals include euhedral to subhedral, locally porphyritic plagioclase as the most common mineral

(33–58 vol. %; crystal cores  $\text{An}_{35-40}$ , rims  $\text{An}_{20}$ ), rare subhedral to anhedral interstitial perthitic K-feldspar (0–12 vol. %), anhedral quartz (22–40 vol. %), subhedral biotite (14–17 vol. %), and locally also secondary (post-magmatic) anhedral muscovite and chlorite after biotite. Accessory minerals (1–3 vol. %) comprise titanite, apatite (hydroxylapatite to fluorapatite), zircon, allanite-(Ce), epidote, magnetite, ilmenite, rutile, and pyrite. Chemical compositions of the studied titanite-bearing granitic rocks are listed in Table 1.

### Titanite description

Titanite forms euhedral to subhedral, dark honey-yellow to pale brown transparent to translucent, wedge-shaped flattened crystals with vitreous to adamantine luster, usually ~0.3 to 10 mm across, in association with plagioclase, quartz, biotite and magnetite (Fig. 2). Tiny inclusions of zircon, apatite, quartz, and biotite were detected in some titanite crystals. The BSE images of titanite crystals often reveal their complex textural growing and dissolution-reprecipitation patterns with domains showing fine oscillatory and sector zoning, in combination with irregular, mosaic or convolute zoning (Fig. 3A–F).

This primary titanite crystals are locally replaced along cleavage planes, fissures and irregular domains by apparently younger quartz, albite, K-feldspar, ilmenite,  $\text{TiO}_2$  phase (rutile and/or anatase), hematite, chlorite, epidote to allanite-(Ce) and secondary titanite, especially in samples from the Veporic Unit (Sihla, Čierna Hora; Fig. 3G–H). Irregular veinlets or chain-like aggregates of the secondary titanite were also

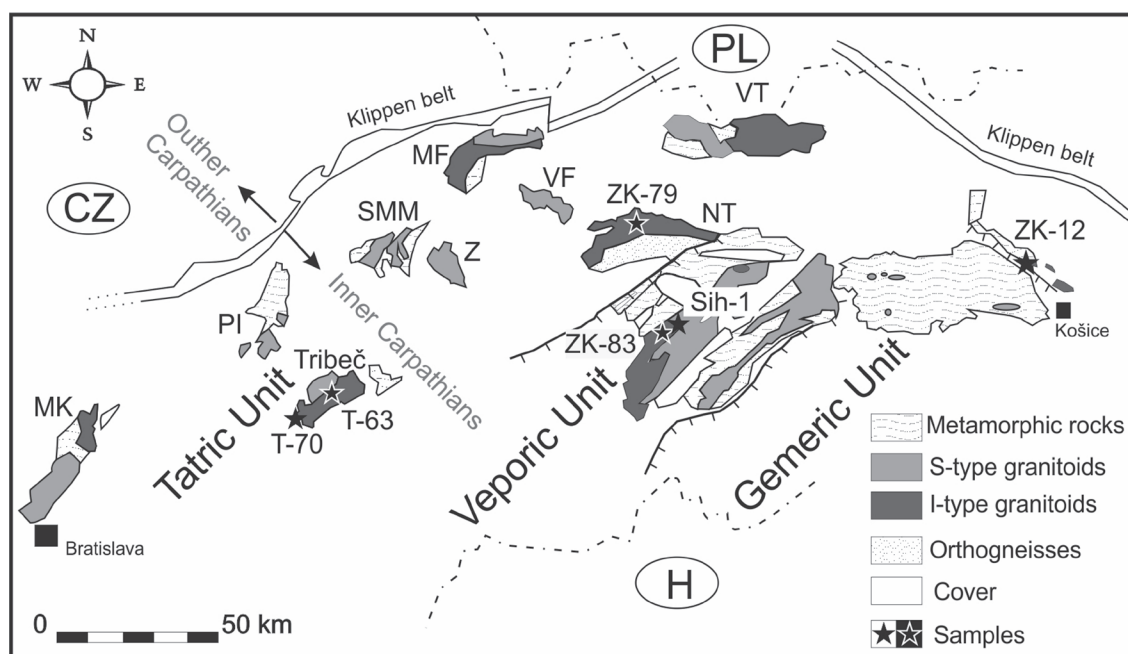


**Fig. 1.** Simplified geological map of the West-Carpathians Paleozoic granitic rocks including titanite-bearing Variscan I-type suite with locations of studied samples: T-63 and T-70 in Tribeč Mts. (Tatric Unit), ZK-79 in Nízke Tatry Mts. (Tatric Unit), ZK-83 and Sih-1 in Vepor Mts. (Veporic Unit) and ZK-12 in Čierna Hora Mts. (Veporic Unit). Abbreviations of mountain areas with granitic massifs in the Tatric Unit: Malé Karpaty (MK), Považský Inovec (PI), Suchý and Malá Magura (SMM), Žiar (Z), Malá Fatra (MF), Veľká Fatra (VF), Vysoké and Západné Tatry (VT), Nízke Tatry (NT); abbreviations of adjacent countries: Czech Republic (CZ), Poland (PL) and Hungary (H).

**Table 1:** Chemical analyses of studied titanite-bearing granitic rocks from the Western Carpathians. Oxides in wt. %, trace elements in ppm. Analytical techniques see Broska & Uher (2001).  $T_{Zrn}$  (°C): zircon saturation temperature in °C (Watson & Harrison 1983).

Sample	T-63	ZK-120 (≈ ZK-79)	VG-14 (≈ ZK-83)	Sih-1	ZK-12
Rock	tonalite	granodiorite	tonalite	tonalite	tonalite
Massif	Tribeč	Prašivá	Vepor	Vepor	Čierna Hora
SiO <sub>2</sub>	64.45	67.79	63.18	64.57	64.34
TiO <sub>2</sub>	0.76	0.46	1.04	0.80	0.93
Al <sub>2</sub> O <sub>3</sub>	16.38	16.12	16.24	16.34	16.18
Fe <sub>2</sub> O <sub>3</sub>	4.45	2.95	4.75	4.29	4.68
MnO	0.08	0.05	0.07	0.07	0.08
MgO	1.86	1.29	1.62	1.62	1.81
CaO	3.46	1.52	3.27	3.59	3.18
Na <sub>2</sub> O	4.15	3.92	4.00	4.36	4.14
K <sub>2</sub> O	2.59	3.88	2.13	2.54	2.47
P <sub>2</sub> O <sub>5</sub>	0.26	0.11	0.43	0.29	0.40
Total	98.44	98.09	96.73	98.47	98.21
Rb	80	139	63	67	67
Sr	848	403	798	860	829
Ba	1237	805	1108	1263	1505
Pb	17	5	3	24	20
Zn	86	71	83	89	85
V	92	53	98	82	97
Cr	26	21	32	18	24
Co	10	6	8	7	34
Ni	9	6	8	4	8
Y	15.24	10.00	37.02	23.01	16.54
La	43.5	29.24	59.43	52.52	59.26
Ce	91.64	60.16	134.06	116.75	118.13
Pr	10.68	6.99	17.05	14.12	13.34
Nd	40.84	26.46	70.44	55.61	49.82
Sm	7.18	4.66	13.56	10.27	8.5
Eu	1.69	1.01	3.19	2.38	2.18
Gd	4.81	3.08	10.36	7.27	6.19
Tb	0.62	0.39	1.42	0.92	0.77
Dy	3.25	2.02	7.57	4.71	3.80
Ho	0.58	0.36	1.40	0.84	0.66
Er	1.54	0.96	3.81	2.42	1.58
Tm	0.21	0.13	0.55	0.36	0.21
Yb	1.34	0.86	3.51	2.19	1.12
Lu	0.19	0.12	0.48	0.32	0.17
Zr	214	136	313	254	290
Hf	4.99	3.21	7.05	5.77	6.41
Nb	10.87	11.95	25.4	19.23	13.16
Ta	0.60	0.82	1.35	1.35	0.99
Th	9.45	10.18	10.39	10.28	9.39
U	5	<	3	4	3
Zr/Hf	42.8	42.4	44.4	44.1	45.3
Ce/Yb	68.4	70.0	38.2	53.3	105.5
ΣREE	223	146	364	294	282
$T_{Zrn}$ (°C)	797	779	840	808	829

described from analogous I-type granitic rocks of the Tribeč Mountains (Broska et al. 2004, 2007). Therefore, their detailed characterization is beyond the scope of this paper.

#### Titanite crystal chemistry

The zoning in BSE reflects variations in the chemical composition of titanite, lighter zones illustrate elevated contents of



**Fig. 2.** Photography of titanite crystals (pale brown, 7 and 5 mm across) in biotite tonalite, Sihla (Sih-1 sample, Vepor Mts.).

Fe and REE's whereas darker zones show higher Ca, Al and/or Ti contents. Aluminium, Fe, REE's (La to Lu+Y) and Nb are the most characteristic isomorphous admixtures of investigated titanite, detected by EPMA (Table 2). Their contents are in the range of 1.0–2.2 wt. % Al<sub>2</sub>O<sub>3</sub> (0.04–0.08 Al atoms per formula unit, *apfu*), 0.6–1.6 wt. % Fe<sub>2</sub>O<sub>3</sub> (0.02–0.04 Fe *apfu*), up to 4.8 wt. % REE<sub>2</sub>O<sub>3</sub> ( $\leq 0.06$  REE *apfu*), and up to 0.5 wt. % Nb<sub>2</sub>O<sub>5</sub> ( $\leq 0.01$  Nb *apfu*). Fluorine content is up to 0.5 wt. % (0.06 F *apfu*). Moreover, slightly decreased analytical totals of measured titanite (usually 97 to 98 wt. %) together with the high contents of Al, Fe, and F indirectly indicate a presence of (OH)<sup>-</sup> anion. The irregular late veinlets and patchy zones of the secondary titanite generally reveal lower contents of Fe ( $\leq 1$  wt. % Fe<sub>2</sub>O<sub>3</sub>), REE ( $\leq 2.5$  wt. % REE<sub>2</sub>O<sub>3</sub>), Nb ( $\leq 0.2$  wt. % Nb<sub>2</sub>O<sub>5</sub>), and atomic Fe/Al ratio (0.2–0.4) (Table 2, anal. 39, 58, 74, and 45) with comparison to the primary zones where the Fe/Al ratio attains 0.4 to 0.8.

The trace-element analyses of titanite by the LA-ICP-MS method reveal a dominance of REE's, especially Y, Ce, and Nd (average contents attain ~1000 to 7500 ppm; ΣREE=6300 to 21200 ppm) over Mg, Mn, Nb, V, Zr, Sn, Th, U (elements with average contents of ~100 to 1300 ppm), and other trace elements with average contents under 100 ppm (Table 3). The REE show a distinct dominance of LREE (La to Sm) over HREE (Gd to Lu, without Y), the average Ce/Yb weight ratio varies between 15 and 51. Chondrite-normalized titanite

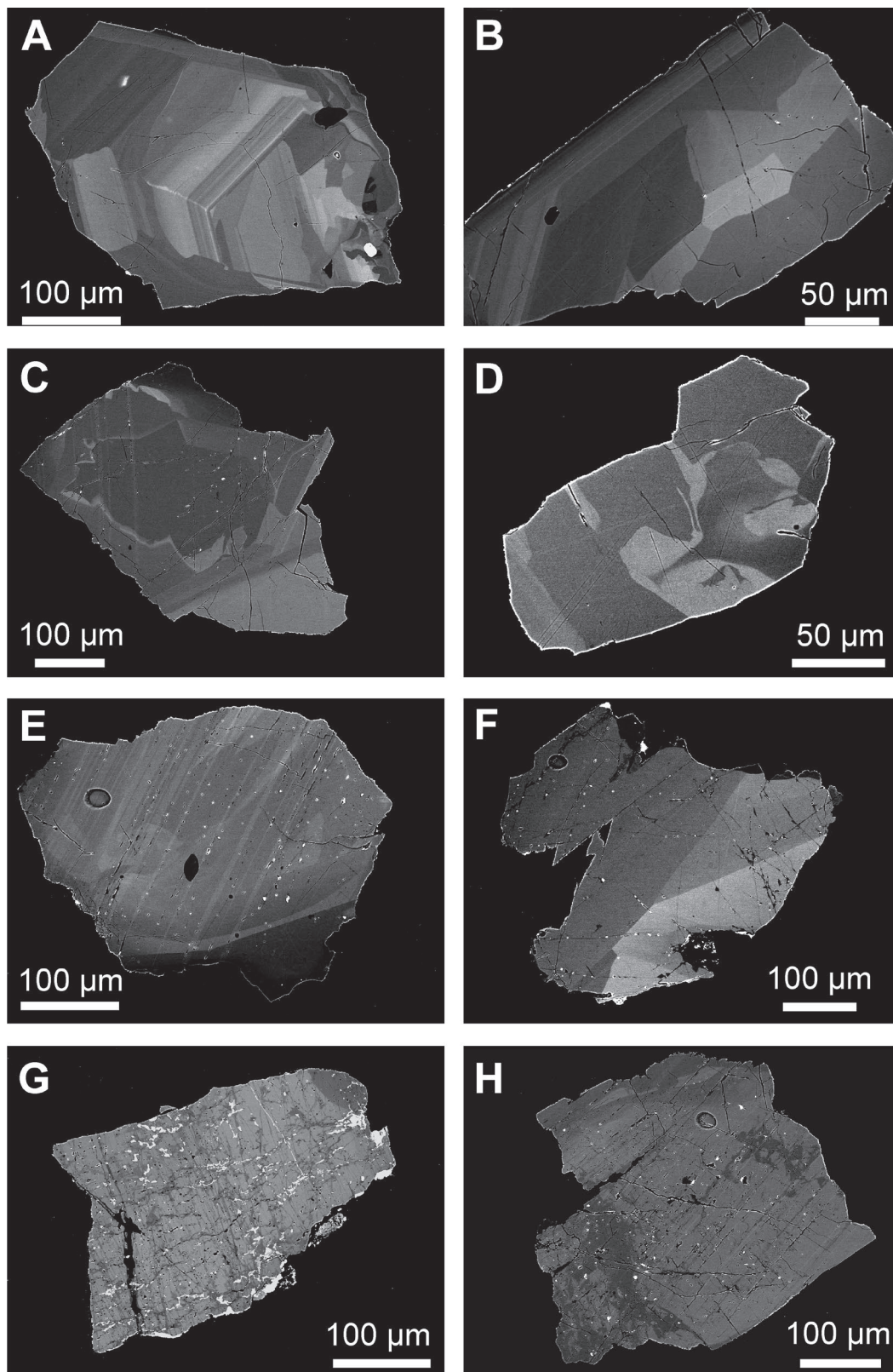


**Fig. 3.** Representative internal textures of titanite from the West-Carpathian granitic rocks (back-scattered electron images, BSE) with various patterns of growth and dissolution–reprecipitation zoning. **A–F:** the combination of fine oscillatory, sector, irregular mosaic and convolute zoning. Zircon (white) forms tiny euhedral inclusion in **A**; **G–H:** primary titanite crystals partly replaced by late (probably Alpine) irregular secondary veinlets and patchy zones of secondary titanite (darker domains) and allanite-(Ce) along cleavage planes, fissures and crystal rims (white small domains and grains). Titanite sample locations: T-63 Tribeč Mts. (**A–B**); T-70 Tribeč Mts. (**C–D**); ZK-79 Nízke Tatry Mts. (**E**); ZK-83 Vepor Mts. (**F**); Sih-1 Vepor Mts. (**G**); ZK-12 Čierna Hora Mts. (**H**).

Table 2: Representative chemical compositions and mineral formulae of studied titanite from the West-Carpathian granitic rocks. Oxides and F in wt. %, mineral formulae in atoms per formula unit (apfu).

Sample	T-63	T-63	T-70	T-70	ZK-79	ZK-79	ZK-79	ZK-83	ZK-83	ZK-83	ZK-83	Sih-1	Sih-1	Sih-1	ZK-12	ZK-12	ZK-12	ZK-12
Analyse	13	15	20	37	39	58	66	68	73	74	80	6A	3B	6B	40	45	52	52
Nb <sub>2</sub> O <sub>5</sub>	0.13	0.14	0.35	0.24	0.11	0.07	0.32	0.21	0.19	0.05	0.44	0.19	0.31	0.20	0.44	0.02	0.66	
SiO <sub>2</sub>	30.29	29.81	29.43	29.93	30.26	30.59	29.75	30.36	30.11	30.32	29.74	30.23	30.01	30.44	29.93	30.40	29.91	
TiO <sub>2</sub>	37.31	35.74	34.75	36.43	36.72	36.36	36.51	36.50	35.98	37.22	36.12	36.08	35.32	38.09	36.42	35.42	36.03	
Al <sub>2</sub> O <sub>3</sub>	1.25	1.27	1.30	1.18	1.25	1.36	1.20	1.50	1.55	1.37	1.44	1.44	1.51	1.27	1.46	2.16	1.36	
Fe <sub>2</sub> O <sub>3</sub>	1.24	1.63	1.54	0.99	1.22	0.67	0.90	1.25	1.29	0.90	1.39	1.46	1.33	0.84	1.16	0.83	1.15	
Y <sub>2</sub> O <sub>3</sub>	0.20	0.66	0.82	0.53	0.14	0.04	0.43	0.57	0.23	0.04	1.14	0.42	0.91	0.77	0.95	0.00	0.62	
La <sub>2</sub> O <sub>3</sub>	0.15	0.13	0.27	0.10	0.16	0.00	0.15	0.00	0.10	0.03	0.07	0.20	0.14	0.00	0.05	0.03	0.07	
Ce <sub>2</sub> O <sub>3</sub>	0.64	0.96	1.46	0.69	0.71	0.05	0.80	0.32	0.47	0.22	0.69	0.86	1.11	0.06	0.44	0.06	0.45	
Pr <sub>2</sub> O <sub>3</sub>	0.05	0.17	0.23	0.15	0.02	0.00	0.14	0.09	0.05	0.01	0.20	0.11	0.27	0.00	0.10	0.00	0.07	
Nd <sub>2</sub> O <sub>3</sub>	0.47	0.97	1.38	0.93	0.37	0.02	0.67	0.38	0.41	0.08	0.98	0.68	1.23	0.34	0.74	0.00	0.50	
Sm <sub>2</sub> O <sub>3</sub>	0.00	0.23	0.35	0.19	0.12	0.03	0.06	0.17	0.21	0.06	0.35	0.12	0.38	0.16	0.31	0.05	0.13	
Gd <sub>2</sub> O <sub>3</sub>	0.04	0.24	0.23	0.23	0.00	0.00	0.08	0.02	0.02	0.14	0.34	0.03	0.34	0.21	0.27	0.03	0.16	
MnO	0.10	0.06	0.13	0.12	0.17	0.05	0.12	0.09	0.09	0.10	0.13	0.17	0.28	0.08	0.18	0.05	0.16	
CaO	27.89	26.64	26.12	26.90	27.71	28.85	26.93	27.97	27.76	28.71	26.45	27.26	26.49	28.07	27.00	28.92	27.76	
Na <sub>2</sub> O	0.00	0.00	0.00	0.00	0.00	0.00	0.00	0.00	0.00	0.03	0.00	0.02	0.00	0.00	0.00	0.00	0.00	
F	0.23	0.19	0.11	0.13	0.09	0.43	0.13	0.37	0.30	0.37	0.06	0.22	0.00	0.20	0.11	0.56	0.05	
Sum (F=O)	99.87	98.74	98.43	98.68	99.00	99.11	98.70	99.68	98.47	99.48	99.51	99.38	99.61	100.63	99.50	98.28	99.04	
REE <sub>2</sub> O <sub>3</sub>	1.54	3.36	4.75	2.82	1.51	0.13	2.44	1.59	1.34	0.58	3.76	2.41	4.37	1.53	2.85	0.16	1.99	

Mineral formulae based on 3 (X+Y+ Si) cations																		
Si	0.994	1.001	0.999	1.002	1.001	1.006	0.999	0.997	0.999	0.992	0.993	1.001	1.002	0.991	0.994	0.999	0.992	
Nb	0.002	0.002	0.005	0.004	0.002	0.001	0.005	0.003	0.003	0.001	0.007	0.003	0.005	0.003	0.007	0.000	0.010	
Ti	0.921	0.902	0.887	0.917	0.913	0.910	0.922	0.902	0.898	0.915	0.907	0.899	0.887	0.933	0.909	0.875	0.898	
Al	0.049	0.050	0.052	0.047	0.049	0.052	0.048	0.058	0.060	0.053	0.057	0.056	0.060	0.049	0.057	0.084	0.053	
Fe	0.031	0.041	0.039	0.025	0.030	0.015	0.023	0.031	0.032	0.022	0.035	0.036	0.033	0.021	0.029	0.020	0.029	
Sum Y	1.002	0.996	0.984	0.993	0.994	0.978	0.997	0.994	0.994	0.991	1.005	0.994	0.985	1.005	1.002	0.980	0.990	
Y	0.003	0.012	0.015	0.009	0.002	0.001	0.008	0.010	0.004	0.001	0.020	0.007	0.016	0.013	0.017	0.000	0.011	
La	0.002	0.002	0.003	0.001	0.002	0.000	0.002	0.000	0.001	0.000	0.001	0.002	0.002	0.000	0.001	0.000	0.001	
Ce	0.008	0.012	0.018	0.008	0.009	0.001	0.010	0.004	0.006	0.003	0.008	0.010	0.014	0.001	0.005	0.001	0.005	
Pr	0.001	0.002	0.003	0.002	0.000	0.000	0.002	0.001	0.001	0.000	0.002	0.001	0.003	0.000	0.001	0.000	0.001	
Nd	0.006	0.012	0.017	0.011	0.004	0.000	0.008	0.005	0.005	0.001	0.012	0.008	0.015	0.004	0.009	0.000	0.006	
Sm	0.000	0.003	0.004	0.002	0.001	0.000	0.002	0.002	0.001	0.001	0.004	0.001	0.004	0.002	0.004	0.001	0.001	
Gd	0.000	0.003	0.003	0.003	0.000	0.000	0.001	0.000	0.000	0.002	0.004	0.000	0.004	0.002	0.003	0.000	0.002	
Mn	0.003	0.002	0.004	0.003	0.005	0.001	0.003	0.003	0.002	0.003	0.004	0.005	0.008	0.002	0.005	0.001	0.005	
Ca	0.981	0.958	0.950	0.965	0.982	1.013	0.969	0.984	0.987	1.006	0.946	0.968	0.948	0.979	0.960	1.018	0.986	
Na	0.000	0.000	0.000	0.000	0.000	0.000	0.000	0.000	0.000	0.002	0.000	0.001	0.000	0.000	0.000	0.000	0.000	
Sum X	1.003	1.004	1.017	1.005	1.016	1.024	1.004	1.009	1.007	1.017	1.001	1.005	1.013	1.004	1.005	1.021	1.018	
Sum REE	0.019	0.044	0.063	0.037	0.019	0.002	0.032	0.022	0.017	0.007	0.051	0.031	0.057	0.022	0.039	0.002	0.027	
F	0.023	0.020	0.012	0.013	0.010	0.045	0.013	0.038	0.031	0.038	0.006	0.023	0.000	0.020	0.011	0.058	0.005	
Fe/Al	0.63	0.82	0.76	0.54	0.63	0.29	0.48	0.53	0.53	0.42	0.62	0.65	0.56	0.42	0.51	0.24	0.54	

Contents of Mg and K were under detection limits.

**Table 3:** Average concentrations of trace elements in titanite from the West-Carpathian granitic rocks (in ppm).

Massif	Tribeč		Nízke Tatry	Vepor		Čierna Hora	Det. lim.
Sample	T-63	T-70	ZK-79	ZK-83	Sih-1	ZK-12	
Li	<	<	<	<	<	<	1.8
Be	<	<	<	<	<	<	2.7
B	<	<	<	<	<	<	47
Mg	174	95	130	124	239	200	2.2
K	28	45	106	79	32	121	10
Sc	25	32	19	22	30	14	2.4
V	862	705	649	698	704	890	1.7
Cr	28	25	28	22	31	47	10
Mn	1342	1131	998	1061	1244	991	5.0
Co	<	<	<	1	<	<	0.4
Ni	<	<	<	<	<	<	11
Cu	<	<	<	<	<	<	8.9
Zn	7.2	7.2	11	14	8.2	17	5.0
Ga	3.6	2.8	2.5	2.4	3.6	3	0.7
As	19	19	17	22	24	15	11
Rb	<	<	<	<	<	<	1.6
Sr	59	45	49	53	51	35	0.3
Y	1678	1942	2050	1526	2682	1222	0.2
Zr	406	285	234	273	357	155	0.1
Nb	1019	850	866	850	1037	932	0.1
Mo	49	29	43	51	50	27	1.5
Cd	<	<	<	<	<	7.8	6.5
In	<	<	<	<	<	<	1.2
Sn	111	110	66	74	118	125	24
Sb	<	<	<	10	<	3.9	2.2
Cs	<	<	<	<	<	<	0.7
Ba	<	<	11	19	<	4.3	2.3
La	2029	1319	705	894	1436	259	0.1
Ce	7479	5594	3370	3918	6570	1393	0.1
Pr	1065	831	628	652	1176	281	0.3
Nd	4822	3779	3343	3333	5580	1468	2.6
Sm	984	713	777	797	1266	423	1.5
Eu	202	158	202	162	208	154	0.9
Gd	597	444	529	519	848	366	3.4
Tb	79	71	75	75	115	59	0.5
Dy	396	398	406	390	592	296	1.5
Ho	75	80	81	70	116	60	0.2
Er	183	204	218	170	277	151	0.6
Tm	23	30	30	21	39	18	0.2
Yb	146	173	189	128	243	95	1.1
Lu	20	21	25	18	31	12	0.2
Hf	35	23	21	20	28	15	1.4
Ta	88	78	65	72	102	47	0.1
W	2.2	1.8	2.1	2.8	1.7	5.7	1.0
Tl	102	<	8.7	<	<	3.8	3.4
Pb	20	13	13	16	17	6.6	0.9
Bi	0.8	2.6	1.3	2.4	0.6	5.1	0.4
Th	580	284	292	298	401	89	0.1
U	118	96	154	169	93	204	0.5
ΣREE	19779	15756	12628	12673	21178	6257	
Ce/Yb	51.2	32.3	17.9	30.6	27.1	14.7	
Y/Ho	22.4	24.3	25.3	21.8	23.0	20.3	
Eu <sub>N</sub> /Eu <sub>N</sub> <sup>*</sup>	0.80	0.85	0.95	0.76	0.61	1.19	
Zr/Hf	11.6	12.1	11.2	13.5	12.6	10.3	
Nb/Ta	11.6	10.9	13.3	11.9	10.2	19.8	

Notes: Det. lim. = lower detection limit (ppm); < = value under the lower detection limit.

$Eu_N/Eu_N^* = Eu_N / \sqrt{(Sm_N * Gd_N)}$ , where  $Eu_N$ ,  $Sm_N$  and  $Gd_N$  are concentrations of Eu, Sm and Gd normalized to chondrite concentrations (after Barrat et al. 2012).

patterns of REE show convex shapes from La to Sm with almost regularly gradual decreasing of HREE's from Gd to Lu, and slightly negative Eu anomalies:  $Eu_N/Eu_N^*$  attains 0.6 to 0.95, with the exception of ZK-12 sample (Čierna Hora) where the value attains 1.2 (Fig. 4). The highest positive correlations between the trace elements of titanite ( $r \geq 0.7$ ) have been observed between Zr vs. Hf,  $\Sigma REE$  vs. Zr (Hf), Th vs. Hf (Zr), and Nb vs. Ta (Fig. 5).

#### Titanite U–Pb dating

The BSE imaging shows that investigated titanite crystals are not homogeneous (Fig. 3) and they are locally slightly porous, but in general, they show sufficiently large unzoned domains for successful in-situ dating (Fig. 6).

The accuracy of the SHRIMP results is strongly influenced by content of uranium in titanite and low U grains usually provide non-accurate results. In consequence, both titanite samples from the Tribeč Mts. (T-63 and T-70) were excluded from the dating, because of their relatively low U contents checked by a single scan of grains on SHRIMP. Finally, only four samples (ZK-79, ZK-83, Sih-1, ZK-12) were analysed. The titanite single spot analyses show compositional variability of U (~40 to ~660 ppm) and Th (~10 to ~680 ppm) in these four samples, used for the dating (Table 4). Contents of Th attain commonly >200 ppm and variable U/Th weight ratio (~1 to 9) appears here. However, in a case of ZK-12 and occasionally also in ZK-79 and ZK-83 samples, a clearly lower Th contents (usually <100 ppm) and corresponding Th/U ratio (~0.1 to 0.6) has been obtained, that may suggest a more complex origin of the parts of crystals.

In the investigated titanite samples, the content of common Pb is moderate to high, ranging from 1.85 % to 29.52 % (Table 4); this table shows also a correlation between common Pb content and discordance. Thus the final age calculations were made for all analyzes as well as after rejection the few highest common Pb results. There are several analyses on titanite crystals in each sample that have concordant or nearly concordant U–Pb ages (+3, –4, –6, +11 % of discordance; Table 4). All from 50 single spot measurements yielded  $^{238}U/^{206}Pb$  age results between  $364 \pm 14$  Ma and  $317 \pm 12$  Ma, but most of them are grouped at 334 Ma with minor peaks at 341 Ma and 349 Ma (based on a histogram plot, not shown).

The age calculations for each sample were conducted for (1) all analysed and then for (2) selected titanite grains, where the lowest common Pb values are <10 % (except Sih-1 sample) were acquired. All calculated values including concordia ages from both Tera–Wasserburg and Wetherill diagrams as well as weighted average  $^{238}U/^{206}Pb$  ages are shown in Table 5 and compared with corresponding zircon ages (Broska et al. 2013). The distribution of data on concordia plots are relatively consistent; results with the lowest MSWD are preferred yielding the following ages (Table 5, Fig. 7):  $343.1 \pm 8.2$  Ma, MSWD=0.47 (Nízke Tatry Mts., ZK-79 sample),  $351.0 \pm 6.5$  Ma, MSWD=0.0047 (Vepor Mts., ZK-83 sample),  $344 \pm 12$  Ma, MSWD=5.9 (Vepor Mts., Sih-1 sample), and  $337.9 \pm 6.1$  Ma,



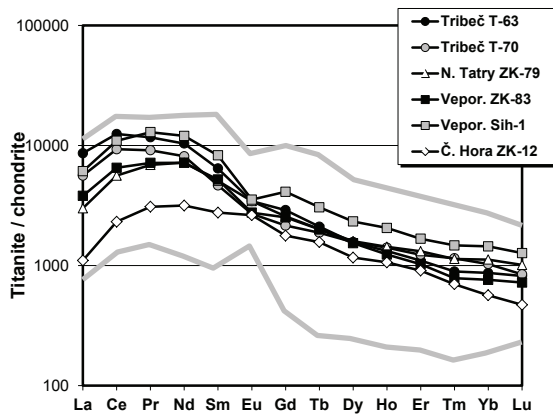


**Fig. 4.** Chondrite-normalized REE patterns of investigated titanite from the West-Carpathian granitic rocks; average REE concentrations in each titanite sample (Table 3) and CI chondrite contents after Barrat et al. (2012) were used.

MSWD=0.85 (Čierna Hora Mts., ZK-12 sample). All these age results are grouped in a relatively narrow, ~13 Ma time interval between 351 and 338 Ma. This age corresponds to Carboniferous, Lower to Middle Mississippian (Tournaisian to Viséan), according to data of the most recent edition of The International Chronostratigraphic Chart (version 2019/05; www.stratigraphy.org).

**Discussion**

*Titanite chemical composition*

Crystal chemistry of titanite allows wide range of various cationic and anionic substitutions, which sensitively reflect geological environment and evolution of the parental rocks. Accessory titanite is an important carrier of REE in granitic

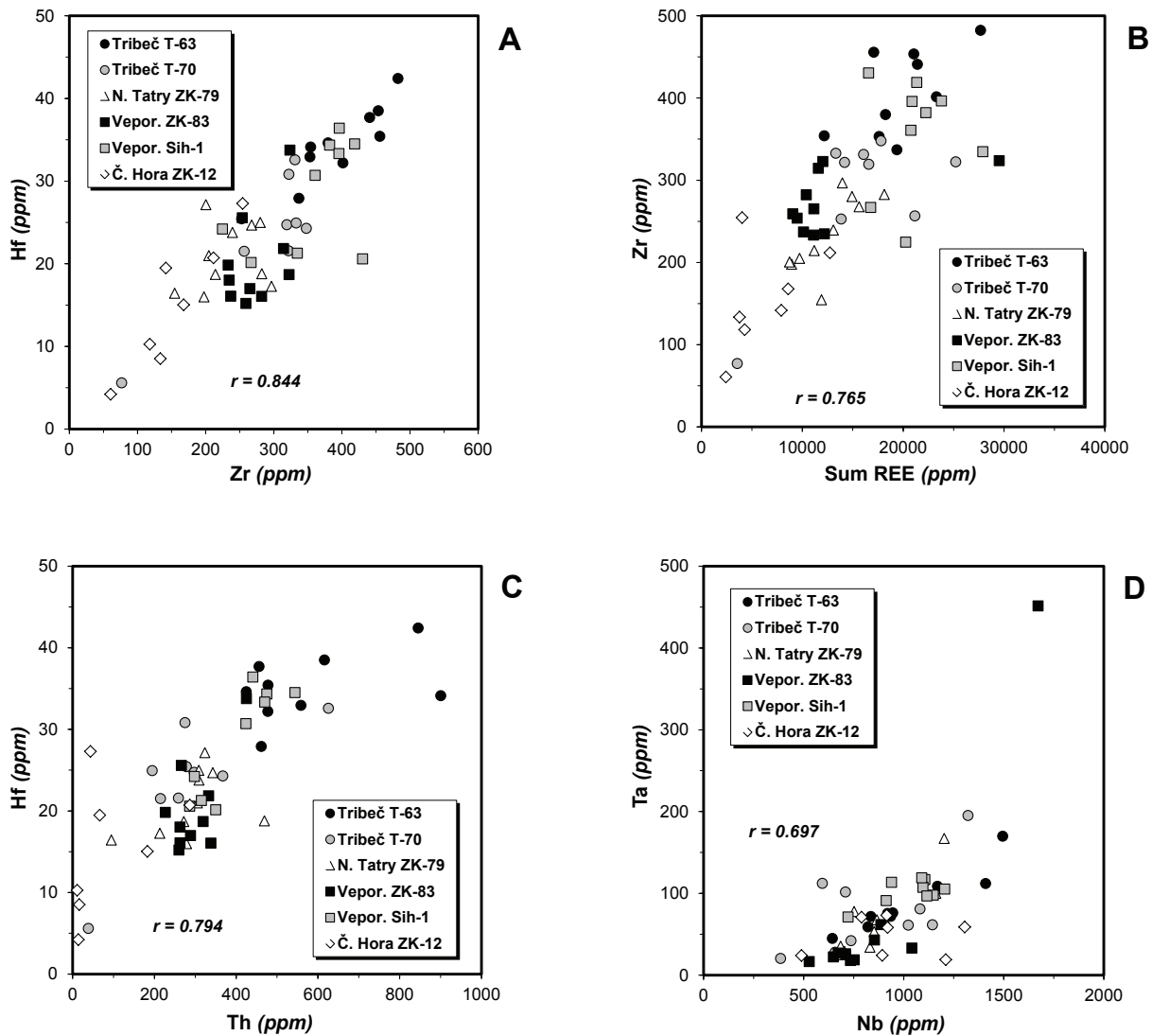


**Fig. 5.** Correlation diagrams of selected trace elements in titanite from the West-Carpathian granitic rocks. The highest positive trace element correlations are illustrated here.

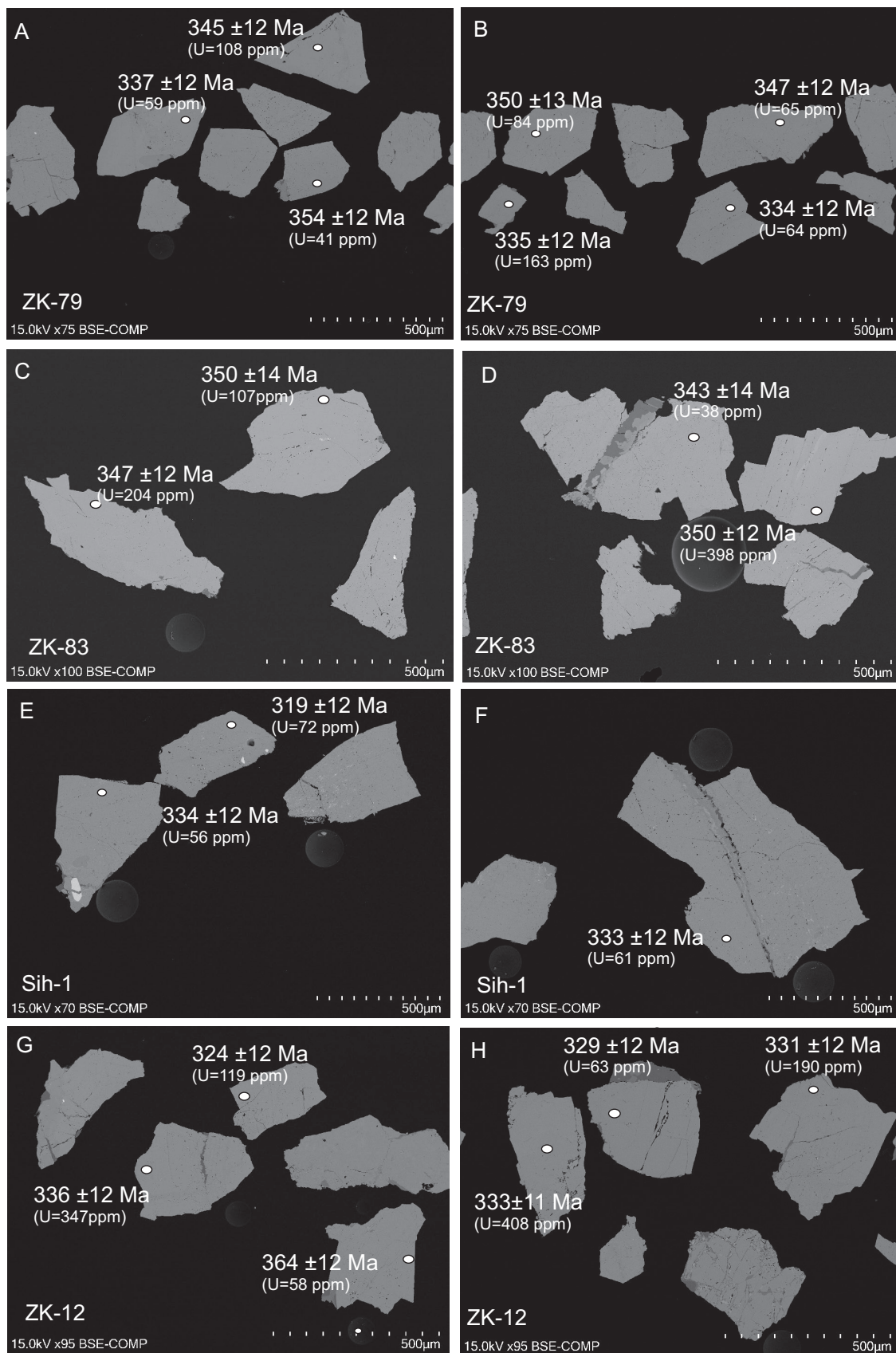
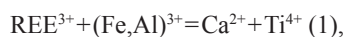


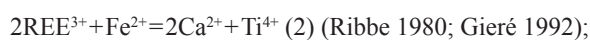
**Fig. 6.** Examples of back-scattered electron (BSE) images of titanite crystal fragments extracted for U–Pb geochronology with age results and corresponding U contents. White ellipses represent locations of spot analyses (20–25 µm in diameter). The age result is also shown. Titanite sample locations: T-79 Nizke Tatry Mts. (A–B); T-83 Vepor Mts. (C–D); Sih-1 Vepor Mts. (E–F); ZK-12 Čierna Hora Mts. (G–H).

rocks, especially in allanite-bearing metaluminous to slightly peraluminous I-type suites, where 80 to 95 wt. % of  $\Sigma$ REE reside in allanite+titanite (Gromet & Silver 1983), and up to 7 wt. % of LREE occupies titanite (Bea 1996). Contents of REE in titanite attain usually up to 5 wt. %  $\text{REE}_2\text{O}_3$  (e.g., Lyakhovich 1968; Higgins & Ribbe 1976; Gromet & Silver 1983; Nakada 1991; Paterson & Stephens 1992; Bea 1996; Della Ventura & Bellatreccia 1999; Hoskin et al. 2000; Chakhmouradian 2004; Vuorinen & Hålenius 2005; Xie et al. 2010). Higher  $\text{REE}_2\text{O}_3$  contents are relatively rare, for example in some titanite crystals in the Ross Mull granite, Scotland, United Kingdom ( $\leq 6.1$  wt. %; McLeod et al. 2011), rhyolitic rocks from Colorado and Nevada, USA ( $\leq 7.4$  wt. %; Ackerson 2011; Colombini et al. 2011), metagranite from the Sulu UHP complex, China ( $\leq 7.6$  wt. %; Chen & Zheng 2015), the Willow Spring Draw rhyolite, New Mexico, USA (8.2 wt. %  $\text{REE}_2\text{O}_3$ ; 2.7 wt. %  $\text{Y}_2\text{O}_3$  and 5.5 wt. % of other  $\text{REE}_2\text{O}_3$ ; Foord et al. 1993). The highest known contents of REE in natural titanite-group minerals are Y-rich titanite (yttrotitanite or keilhauite variety) with 12.1 wt. %  $\text{REE}_2\text{O}_3$ , 6.2 wt. %  $\text{Al}_2\text{O}_3$  and 5.9 wt. %  $\text{Fe}_2\text{O}_3$  from Buöe (Boie) granitic pegmatite near Arendal, Norway (Vlasov et al. 1964) and natrotitanite  $[(\text{Na}_{0.5}\text{Y}_{0.5})\text{Ti}(\text{SiO}_4)\text{O}]$ , a member of titanite group with 18.5 wt. % of  $\text{REE}_2\text{O}_3$  from the Verkhnee Espe rare-element deposit, Kazakhstan, related to alkaline granites (Stepanov et al. 2012).

The REE's together with Al and Fe are dominant cation isomorphic admixtures in the studied titanite ( $\leq 4.8$  wt. %  $\text{REE}_2\text{O}_3$ , 1.0–2.2 wt. %  $\text{Al}_2\text{O}_3$ , 0.6–1.6 wt. %  $\text{Fe}_2\text{O}_3$ ; Table 1). Following principal coupled substitution mechanisms drive entry of REE's, Al and Fe into titanite structure:



in REE-(Fe,Al)-rich and Na-poor titanite, typical mainly for granitic rocks (e.g., Zabavnikova 1957; Vlasov et al. 1964; Lyakhovich 1968; Ribbe 1980; Green & Pearson 1986; Broska et al. 2004), rarely in alkaline pegmatites (Russell et al. 1994);



$\text{Na}^+ + (\text{Y, HREE})^{3+} = 2\text{Ca}^{2+}$  (3), found in natrotitanite (Stepanov et al. 2012);

$(\text{Al,Fe})^{3+} + (\text{OH,F})^- = \text{Ti}^{4+} + \text{O}^{2-}$  (4), substitution typical mainly for metamorphic titanite (e.g., Zabavnikova 1957; Ribbe 1980; Green & Pearson 1986; Gieré 1992; Chen & Zheng 2015);

$\text{Fe}^{2+} + 2(\text{OH, F})^- = \text{Ti}^{4+} + 2\text{O}^{2-}$  (5) (Zabavnikova 1957; Gieré 1992), and

$\text{Fe}^{2+} + \text{vacancy} = \text{Ti}^{4+} + \text{O}^{2-}$  (6) substitution (Gieré 1992).

The  $^{57}\text{Fe}$  Mössbauer spectroscopy indicates a general dominance of  $\text{Fe}^{3+}$  over  $\text{Fe}^{2+}$  in titanite from the West-Carpathian granitic rocks with 13.5 to 22.0 %  $\text{Fe}^{2+}$  [ $100 \cdot \text{Fe}^{2+} / (\text{Fe}^{2+} + \text{Fe}^{3+})$ ]; however some titanite samples (Nitra and Sihla) show 43.6 and 58.3 %  $\text{Fe}^{2+}$ , respectively (Broska et al. 2004). Therefore,

the entry of REE into the titanite structure is compensated by both  $\text{Fe}^{3+}$  and  $\text{Fe}^{2+}$  cations along the (1) and (2) substitution mechanisms in the studied samples. The REE versus  $\text{Fe}_{\text{total}}$  ( $\text{Fe}^{2+} + \text{Fe}^{3+}$ ) diagram shows positive correlation trend with atomic REE:Fe ratio between 2:1 and 1:1, which also support the presence of both iron valence states in titanite (Fig. 8A). Moreover, some compositions reveal the REE:Fe ratio below 1:1, indicating a presence of other substitution mechanisms including Fe without REE, mainly (4) exchange (Fig. 8A–B).

Entry of  $\text{Nb}^{5+}$  cation into the structure of investigated titanite (up to 0.5 wt. %  $\text{Nb}_2\text{O}_5$ ) could be compensated by trivalent cations along the  $\text{Nb}^{5+} + (\text{Al,Fe})^{3+} = 2\text{Ti}^{4+}$  substitution vector (7), to zabińskiite end-member,  $\text{Ca}(\text{Al}_{0.5}\text{Ta}_{0.5})(\text{SiO}_4)\text{O}$  (Piecicka et al. 2017). However, measured contents of Nb and Ta in the studied West-Carpathian titanites are too low for unambiguous evidence of such a mechanism.

The major and trace element composition of titanite can discriminate their magmatic versus metamorphic or hydrothermal origin. Generally, the Fe/Al atomic ratio over 0.5 corresponds to titanite from igneous rocks, conversely values  $< 0.5$  are characteristic for metamorphic titanite (Nakada 1991; Kowallis et al. 1997, 2018; Aleinikoff et al. 2002). The Fe/Al ratio of investigated titanite attains 0.4–0.8 for primary REE- and Fe-enriched domains in contrast to 0.2–0.4 in the secondary REE- and Fe-poor titanite. Therefore, the Fe/Al value is not unambiguous for primary titanite but it indicates metamorphic (non-igneous) origin of secondary titanite zones. Higher Th/U weight ratio ( $\sim 1$  to 9) in majority of measured titanite crystals reveals rather a magmatic origin of titanite in contrast to distinctly lower Th/U ratio ( $\sim 0.1$  to 0.6) in some domains (especially in ZK-12 sample), probably of secondary titanite which indicate metamorphic or hydrothermal origin (cf. Aleinikoff et al. 2002; Li et al. 2010; Gao et al. 2012). However, the Th/U ratio cannot effectively discriminates igneous vs. hydrothermal or metamorphic source for high-temperature titanite (Liu et al. 2018).

The chondrite-normalized pattern of studied titanite, consisting convex shape of LREE, insignificant to absent Eu anomaly and gradual decreasing of HREE (Fig. 4) also is not an efficient discriminator for igneous vs. metamorphic or hydrothermal origin. Analogous REE-normalized patterns display titanite from granitic rocks (Bea 1996; Bauer 2015; Kohn 2017) as well as from metamorphic rocks (eclogites; Gao et al. 2011; Skublov et al. 2014). Consequently, the shape of the chondrite-normalized REE patterns of titanite is rather a result of different REE partitioning between the host-rock minerals.

#### ***Titanite age and origin***

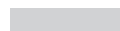
Titanite is a relatively common accessory mineral and a principal carrier of titanium in the West-Carpathian Variscan I-type tonalites to granodiorites; it fixes  $\leq 80$  wt. % Ti of the bulk rock (Broska et al. 2004). Titanite is here present in the association of magnetite+quartz, which indicates a relatively increased oxygen fugacity ( $\log f\text{O}_2 \approx -12$ ).

**Table 4:** Isotope U, Th, and Pb data of studied titanite from the West-Carpathian granitic rocks.

spot	<sup>204</sup> Pb/ <sup>206</sup> Pb ± %	<sup>207</sup> Pb/ <sup>206</sup> Pb ± %	<sup>208</sup> Pb/ <sup>206</sup> Pb ± %	<sup>206</sup> Pb/ <sup>238</sup> U ± %	<sup>206</sup> Pb/ <sup>254</sup> UO ± %	corrected <sup>204</sup> Pb/ <sup>206</sup> Pb	<sup>206</sup> Pb <sub>c</sub> %	U ppm	Th ppm	Th/U	corrected <sup>206</sup> Pb* ppm					
<b>ZK-79: granodiorite, Brusno, Nizke Tatry Mountains</b>																
ZK-79.1.1	0.00823	5.3	0.181	2.5	0.944	1.1	1.612	4.7	0.1040	2.1	0.0087	15.98	78	231	2.96	3.4
ZK-79.2.1	0.00924	6.7	0.190	7.7	1.306	1.8	1.559	5.6	0.1078	4.0	0.0093	17.07	65	304	4.68	3.1
ZK-79.3.1	0.00479	9.6	0.129	1.7	1.052	0.6	1.849	2.5	0.1107	0.9	0.0052	9.42	53	222	4.19	2.4
ZK-79.4.1	0.00435	8.4	0.116	1.0	0.914	0.6	1.521	3.4	0.1009	1.5	0.0043	7.81	81	276	3.41	3.9
ZK-79.5.1	0.00530	8.1	0.135	2.8	1.049	0.6	1.703	2.8	0.1059	1.1	0.0056	10.21	64	256	4.00	2.9
ZK-79.6.1	0.01240	4.4	0.222	5.4	1.288	3.8	1.890	6.2	0.1203	5.2	0.0115	21.11	61	291	4.77	2.9
ZK-79.7.1	0.00457	8.0	0.115	1.0	0.887	0.6	1.530	2.8	0.1017	1.4	0.0042	7.71	84	277	3.30	4.0
ZK-79.8.1	0.00317	5.5	0.101	1.5	0.181	3.0	1.652	3.2	0.1023	1.4	0.0032	5.94	163	39	0.24	7.5
ZK-79.9.1	0.00277	10.0	0.101	0.9	0.433	0.6	1.561	2.4	0.1008	1.1	0.0032	5.93	108	151	1.40	5.1
ZK-79.10.1	0.00830	7.9	0.177	1.1	0.442	1.1	1.684	4.8	0.1120	2.4	0.0085	15.47	41	24	0.59	2.0
ZK-79.11.1	0.00495	8.9	0.129	1.0	1.154	0.6	1.718	1.9	0.1065	1.2	0.0052	9.51	59	265	4.49	2.7
ZK-79.12.1	0.00762	6.5	0.169	2.7	1.829	0.5	1.708	3.2	0.1129	1.7	0.0079	14.47	65	477	7.34	3.2
ZK-79.13.1	0.00450	8.5	0.117	1.0	0.903	0.6	1.628	2.1	0.1026	1.1	0.0044	7.98	74	250	3.38	3.4
ZK-79.14.1	0.00537	9.2	0.134	1.0	1.041	0.6	1.829	2.3	0.1127	1.7	0.0055	10.06	53	205	3.87	2.5
ZK-79.15.1	0.00512	8.0	0.132	0.9	1.004	0.6	1.774	3.0	0.1098	1.3	0.0053	9.78	64	239	3.73	3.0
<b>ZK-83: tonalite, Hriňová, Slovenské Rudohorie Mountains</b>																
ZK-83.1.1	0.00190	7.9	0.082	0.7	0.336	0.5	1.488	1.9	0.0976	0.9	0.0020	3.62	204	231	1.13	9.7
ZK-83.2.1	0.00304	7.9	0.096	0.8	0.632	0.5	1.643	2.3	0.1034	0.4	0.0029	5.28	107	244	2.28	5.1
ZK-83.3.1	0.00642	4.5	0.142	5.6	0.584	3.7	1.660	3.8	0.1068	1.2	0.0061	11.08	115	187	1.63	5.4
ZK-83.4.1	0.00092	7.5	0.069	1.2	0.086	2.6	1.496	3.2	0.0973	1.3	0.0010	1.88	398	77	0.19	19.1
ZK-83.5.1	0.00528	7.5	0.129	0.9	0.960	0.6	1.821	3.2	0.1126	1.4	0.0051	9.40	58	210	3.62	2.8
ZK-83.6.1	0.00630	6.4	0.145	1.8	0.942	0.6	1.633	3.8	0.1087	1.6	0.0062	11.42	77	253	3.29	3.8
ZK-83.7.1	0.00099	7.4	0.068	0.5	0.070	0.8	1.603	2.9	0.0998	1.3	0.0010	1.85	338	45	0.13	15.9
ZK-83.8.1	0.00741	6.5	0.156	4.7	0.899	2.4	1.881	3.0	0.1124	1.5	0.0071	12.91	56	174	3.11	2.5
ZK-83.9.1	0.00467	5.9	0.124	8.2	0.622	2.5	1.584	3.9	0.1025	1.9	0.0048	8.82	113	223	1.97	5.2
ZK-83.10.1	0.00826	7.2	0.196	3.8	0.428	4.0	1.886	3.5	0.1182	1.7	0.0097	17.78	38	10	0.26	1.8
ZK-83.11.1	0.00643	4.4	0.137	5.7	0.640	2.1	1.737	4.0	0.1093	2.3	0.0057	10.51	109	215	1.97	5.1
ZK-83.12.1	0.00752	7.0	0.169	2.6	0.981	0.6	1.831	3.6	0.1159	1.6	0.0079	14.42	63	216	3.43	3.0
ZK-83.13.1	0.00514	8.5	0.125	1.0	1.050	0.6	1.692	2.5	0.1076	1.4	0.0049	8.90	65	255	3.92	3.1
ZK-83.14.1	0.00134	7.7	0.073	1.5	0.084	1.3	1.455	3.5	0.0974	1.4	0.0013	2.37	305	44	0.14	14.9
ZK-83.15.1	0.00694	6.6	0.156	4.6	1.114	0.6	1.935	2.4	0.1174	1.1	0.0070	12.85	54	229	4.24	2.6
<b>Sih-1: tonalite, Sihla, Slovenské Rudohorie Mountains</b>																
Sih-1.1.1	0.00704	6.4	0.165	2.5	1.326	0.5	1.643	4.4	0.1080	2.6	0.0076	13.98	72	381	5.29	3.4
Sih-1.1.2	0.00518	8.7	0.141	0.9	1.237	0.6	1.833	2.7	0.1104	1.6	0.0060	11.03	56	272	4.86	2.6
Sih-1.2.1	0.00532	8.7	0.135	1.0	1.350	0.6	1.667	3.2	0.1045	1.4	0.0056	10.27	61	338	5.54	2.8
Sih-1.3.1	0.01585	4.1	0.289	3.1	1.387	0.6	1.623	3.8	0.1064	1.7	0.0161	29.52	64	261	4.08	2.4
Sih-1.4.1	0.01314	4.6	0.244	1.4	2.176	0.5	1.539	2.8	0.1070	1.1	0.0130	23.83	72	678	9.42	3.1
Sih-1.5.1	0.00534	8.2	0.143	0.9	1.308	0.5	1.803	2.8	0.1097	1.6	0.0061	11.19	58	305	5.26	2.7
<b>ZK-12 tonalite, Kysak, Čierna Hora Mountains</b>																
ZK-12.1.1	0.00142	7.3	0.075	0.6	0.102	0.8	1.524	2.5	0.0967	0.9	0.0015	2.72	341	75	0.22	15.7
ZK-12.2.1	0.00910	3.9	0.176	2.9	0.642	0.6	1.652	2.7	0.1061	1.5	0.0084	15.43	119	209	1.76	5.3
ZK-12.3.1	0.01265	5.7	0.234	1.0	0.521	2.3	1.466	3.6	0.1108	1.5	0.0123	22.58	58	9	0.16	2.9
ZK-12.4.1	0.00105	8.5	0.070	1.1	0.077	0.8	1.443	3.4	0.0937	1.1	0.0011	2.05	347	51	0.15	15.9
ZK-12.5.1	0.00131	4.8	0.074	0.4	0.088	1.2	1.385	4.2	0.0923	1.7	0.0014	2.56	658	97	0.15	30.4
ZK-12.6.1	0.00271	6.2	0.090	0.7	0.292	0.5	1.655	2.0	0.0994	0.9	0.0026	4.70	178	156	0.88	7.8
ZK-12.7.1	0.00369	5.8	0.103	0.7	0.209	0.7	1.532	4.0	0.0972	2.0	0.0034	6.24	144	52	0.36	6.4
ZK-12.8.1	0.00150	4.8	0.075	1.1	0.069	1.9	1.420	4.3	0.0935	1.8	0.0015	2.69	558	30	0.05	25.7
ZK-12.9.1	0.00143	6.9	0.075	1.4	0.087	2.7	1.517	3.3	0.0972	1.3	0.0015	2.75	310	41	0.13	14.5
ZK-12.10.1	0.00143	9.4	0.077	0.7	0.301	0.5	1.494	2.9	0.0957	1.2	0.0016	2.92	249	255	1.02	11.4
ZK-12.11.1	0.00177	5.8	0.081	4.2	0.160	6.5	1.379	3.7	0.0919	1.6	0.0019	3.45	408	154	0.38	18.6
ZK-12.12.1	0.00524	7.4	0.139	0.9	0.268	1.0	1.696	3.1	0.1053	1.5	0.0058	10.69	63	14	0.22	2.8
ZK-12.13.1	0.00423	4.8	0.115	2.0	0.210	2.5	1.432	3.9	0.0955	1.7	0.0042	7.72	190	39	0.21	8.6
ZK-12.14.1	0.00348	7.5	0.101	0.8	0.391	1.4	1.622	2.2	0.1017	1.4	0.0033	6.02	107	129	1.21	5.0
ZK-12.15.1	0.00487	6.2	0.129	0.7	0.458	0.6	1.701	2.1	0.1050	0.8	0.0052	9.46	110	138	1.25	5.0

Errors are 1-sigma; Pb<sub>c</sub> and Pb\* indicate the common and radiogenic portions, respectively.

Error in standard calibration was 0.81 % (not included in above errors but required when comparing data from different mounts).

 isotopic ratio selected to concordia calculation

**Table 4 (continued):** Isotope U, Th, and Pb data of studied titanite from the West-Carpathian granitic rocks.

spot	corrected <sup>208</sup> Pb <sup>+</sup> ppm	<sup>232</sup> Th/ <sup>238</sup> U ± %	<sup>206</sup> Pb/ <sup>238</sup> U age (Ma)	<sup>207</sup> Pb/ <sup>206</sup> Pb age (Ma)	discordant %	<sup>238</sup> U/ <sup>206</sup> Pb <sup>+</sup> ± %	<sup>207</sup> Pb <sup>+</sup> / <sup>206</sup> Pb <sup>+</sup> ± %	<sup>207</sup> Pb/ <sup>235</sup> U ± %	<sup>206</sup> Pb <sup>+</sup> / <sup>238</sup> U ± %	error corr.					
<b>ZK-79: granodiorite, Brusno, Nizke Tatry Mountains</b>															
ZK-79.1.1	2.5	3.1	317 ± 12	653 ± 322	52	19.61	4.0	0.0614	15.0	0.432	15.5	0.0510	4.0	0.3	
ZK-79.2.1	3.6	4.8	1.6	347 ± 17	411 ± 844	11	18.05	4.6	0.0550	37.7	0.420	38.0	0.0554	4.6	0.1
ZK-79.3.1	2.3	4.3	0.7	338 ± 12	564 ± 285	41	18.46	3.8	0.0589	13.1	0.440	13.6	0.0542	3.8	0.3
ZK-79.4.1	3.2	3.5	1.1	347 ± 13	291 ± 261	-19	18.12	3.8	0.0521	11.4	0.397	12.0	0.0552	3.8	0.3
ZK-79.5.1	2.8	4.1	0.7	334 ± 12	518 ± 305	36	18.70	3.8	0.0577	13.9	0.425	14.4	0.0535	3.8	0.3
ZK-79.6.1	3.1	4.9	1.2	343 ± 23	-556 ± 1371	165	18.65	6.7	0.0370	50.9	0.274	51.4	0.0536	6.7	0.1
ZK-79.7.1	3.2	3.4	1.0	350 ± 13	90 ± 296	-295	18.03	3.8	0.0478	12.5	0.366	13.0	0.0555	3.8	0.3
ZK-79.8.1	0.5	0.2	1.5	335 ± 12	387 ± 131	9	18.69	3.6	0.0544	5.9	0.401	6.9	0.0535	3.6	0.5
ZK-79.9.1	1.7	1.5	0.8	345 ± 12	627 ± 154	46	18.03	3.7	0.0607	7.1	0.464	8.0	0.0554	3.7	0.5
ZK-79.10.1	0.3	0.6	1.6	354 ± 13	466 ± 451	25	17.68	4.1	0.0563	20.4	0.439	20.8	0.0566	4.1	0.2
ZK-79.11.1	2.9	4.6	0.6	337 ± 12	498 ± 278	33	18.53	3.8	0.0572	12.6	0.425	13.2	0.0540	3.8	0.3
ZK-79.12.1	5.7	7.6	1.0	359 ± 13	550 ± 369	35	17.35	3.9	0.0585	16.9	0.465	17.3	0.0576	3.9	0.2
ZK-79.13.1	2.7	3.5	0.2	335 ± 12	238 ± 284	-42	18.83	3.8	0.0509	12.3	0.373	12.9	0.0531	3.8	0.3
ZK-79.14.1	2.4	4.0	1.2	351 ± 13	434 ± 325	16	17.83	3.9	0.0555	14.6	0.429	15.1	0.0561	3.9	0.3
ZK-79.15.1	2.7	3.9	1.0	345 ± 13	491 ± 259	30	18.10	3.8	0.0570	11.7	0.434	12.3	0.0553	3.8	0.3
<b>ZK-83: tonalite, Hriňová, Slovenské Rudohorie Mountains</b>															
ZK-83.1.1	2.7	1.2	0.5	347 ± 12	398 ± 97	12	18.03	3.6	0.0547	4.3	0.418	5.6	0.0555	3.6	0.6
ZK-83.2.1	2.9	2.3	3.0	350 ± 14	248 ± 172	-42	17.95	4.0	0.0512	7.5	0.393	8.5	0.0557	4.0	0.5
ZK-83.3.1	2.2	1.7	1.6	343 ± 14	67 ± 518	-419	18.43	4.1	0.0474	21.7	0.354	22.1	0.0542	4.1	0.2
ZK-83.4.1	0.9	0.2	1.7	350 ± 12	414 ± 55	16	17.90	3.6	0.0550	2.4	0.424	4.4	0.0559	3.6	0.8
ZK-83.5.1	2.4	3.8	0.8	354 ± 13	252 ± 295	-41	17.77	3.8	0.0512	12.8	0.398	13.4	0.0563	3.8	0.3
ZK-83.6.1	3.0	3.4	1.7	360 ± 13	319 ± 314	-9	17.42	3.8	0.0528	13.8	0.418	14.3	0.0574	3.8	0.3
ZK-83.7.1	0.5	0.1	0.9	344 ± 12	355 ± 49	3	18.22	3.6	0.0536	2.2	0.406	4.2	0.0549	3.6	0.9
ZK-83.8.1	1.8	3.2	0.8	328 ± 13	48 ± 600	-594	19.27	4.1	0.0470	25.1	0.336	25.4	0.0519	4.1	0.2
ZK-83.9.1	2.5	2.0	1.1	340 ± 13	440 ± 475	23	18.42	3.7	0.0557	21.4	0.417	21.7	0.0543	3.7	0.2
ZK-83.10.1	0.1	0.3	0.7	343 ± 13	1159 ± 334	71	17.70	4.0	0.0785	16.9	0.611	17.3	0.0565	4.0	0.2
ZK-83.11.1	2.4	2.0	0.8	345 ± 13	-232 ± 604	253	18.44	3.7	0.0419	24.0	0.313	24.2	0.0542	3.7	0.2
ZK-83.12.1	2.4	3.6	1.2	353 ± 13	592 ± 372	41	17.64	3.9	0.0597	17.2	0.467	17.6	0.0567	3.9	0.2
ZK-83.13.1	3.0	4.1	1.1	351 ± 13	151 ± 347	-135	17.98	3.8	0.0491	14.8	0.376	15.3	0.0556	3.8	0.2
ZK-83.14.1	0.5	0.1	0.4	357 ± 13	326 ± 82	-10	17.56	3.6	0.0529	3.6	0.416	5.1	0.0569	3.6	0.7
ZK-83.15.1	2.5	4.4	0.8	350 ± 13	402 ± 461	12	17.91	3.9	0.0548	20.6	0.421	20.9	0.0558	3.9	0.2
<b>Sih-1: tonalite, Sihla, Slovenské Rudohorie Mountains</b>															
Sih-1.1.1	4.1	5.4	3.3	344 ± 14	723 ± 298	53	18.03	4.1	0.0634	14.0	0.485	14.6	0.0555	4.1	0.3
Sih-1.1.2	2.9	5.0	1.2	334 ± 12	834 ± 229	61	18.47	3.8	0.0669	11.0	0.499	11.6	0.0541	3.8	0.3
Sih-1.2.1	3.6	5.7	2.4	333 ± 12	522 ± 288	37	18.78	3.8	0.0578	13.1	0.424	13.7	0.0533	3.8	0.3
Sih-1.3.1	2.7	4.2	1.6	278 ± 11	520 ± 697	47	22.56	4.1	0.0578	31.8	0.353	32.0	0.0443	4.1	0.1
Sih-1.4.1	7.0	9.7	0.2	319 ± 12	220 ± 577	-46	19.77	4.0	0.0505	24.9	0.353	25.3	0.0506	4.0	0.2
Sih-1.5.1	3.2	5.4	1.1	334 ± 12	798 ± 227	59	18.51	3.8	0.0658	10.8	0.490	11.5	0.0540	3.8	0.3
<b>ZK-12 tonalite, Kysak, Čierna Hora Mountains</b>															
ZK-12.1.1	0.7	0.2	3.6	336 ± 12	379 ± 68	10	18.65	3.7	0.0542	3.0	0.401	4.7	0.0536	3.7	0.8
ZK-12.2.1	2.0	1.8	1.0	324 ± 12	-283 ± 549	219	19.67	3.7	0.0411	21.6	0.288	21.9	0.0508	3.7	0.2
ZK-12.3.1	0.2	0.2	0.9	364 ± 14	93 ± 697	-295	17.34	4.1	0.0479	29.4	0.381	29.7	0.0577	4.1	0.1
ZK-12.4.1	0.6	0.2	1.2	335 ± 12	379 ± 64	11	18.71	3.7	0.0542	2.8	0.399	4.7	0.0534	3.7	0.8
ZK-12.5.1	1.1	0.2	1.6	337 ± 12	393 ± 41	14	18.59	3.7	0.0545	1.8	0.404	4.1	0.0538	3.7	0.9
ZK-12.6.1	1.6	0.9	0.6	321 ± 11	227 ± 121	-42	19.64	3.6	0.0507	5.3	0.356	6.4	0.0509	3.6	0.6
ZK-12.7.1	0.5	0.4	1.0	326 ± 12	129 ± 168	-156	19.38	3.7	0.0486	7.1	0.346	8.0	0.0516	3.7	0.5
ZK-12.8.1	0.3	0.1	1.7	337 ± 12	317 ± 60	-6	18.65	3.6	0.0527	2.6	0.390	4.5	0.0536	3.6	0.8
ZK-12.9.1	0.4	0.1	0.8	341 ± 12	385 ± 75	10	18.38	3.6	0.0543	3.4	0.408	4.9	0.0544	3.6	0.7
ZK-12.10.1	2.9	1.1	1.3	336 ± 12	436 ± 83	23	18.66	3.6	0.0556	3.7	0.411	5.2	0.0536	3.6	0.7
ZK-12.11.1	1.7	0.4	0.7	333 ± 12	402 ± 158	18	18.84	3.6	0.0548	7.1	0.401	7.9	0.0531	3.6	0.5
ZK-12.12.1	0.1	0.2	0.6	329 ± 12	700 ± 217	54	18.89	3.8	0.0628	10.2	0.458	10.9	0.0530	3.8	0.3
ZK-12.13.1	0.5	0.2	0.9	331 ± 12	319 ± 176	-4	18.99	3.6	0.0528	7.8	0.383	8.6	0.0527	3.6	0.4
ZK-12.14.1	1.4	1.2	0.4	338 ± 12	207 ± 194	-65	18.64	3.7	0.0503	8.4	0.372	9.2	0.0536	3.7	0.4
ZK-12.15.1	1.4	1.3	0.5	331 ± 12	524 ± 186	37	18.87	3.7	0.0578	8.5	0.423	9.3	0.0530	3.7	0.4

**Table 5:** The U–Pb age results of titanite (this study) and zircon (Broska et al. 2013) calculated by Tera–Wasserburg (T–W), Wetherill (W) and Mean U–Pb methods. Preferred results are written in bold font.

Sample	age (Ma)	±(Ma)	MSWD	N	calculation
<i>Titanite (this study)</i>					
ZK-79	343.7	6.8	1.4	15	T–W
(Nízke Tatry Mts.)	<b>343.1</b>	<b>8.2</b>	<b>0.47</b>	<b>8</b>	<b>W</b>
	341.8	5.8	0.60	15	Mean U–Pb
ZK-83	348.5	6.6	0.31	15	T–W
(Vepor Mts.)	<b>351.0</b>	<b>6.5</b>	<b>0.0047</b>	<b>12</b>	<b>W</b>
	347.8	6.5	0.42	15	Mean U–Pb
Sih-1	336	11	6.5	5	T–W
(Vepor Mts.)	<b>344</b>	<b>12</b>	<b>5.9</b>	<b>4</b>	<b>W</b>
	340	13	0.18	4	Mean U–Pb
ZK-12	334.9	6.2	1.7	15	T–W
(Čierna Hora Mts.)	<b>337.9</b>	<b>6.1</b>	<b>0.85</b>	<b>10</b>	<b>W</b>
	334.0	6.1	0.59	15	Mean U–Pb
<i>Zircon (Broska et al. 2013; *recalculated)</i>					
NTBS-2	353	3	1.6	11	T–W
(Nízke Tatry Mts.)	<b>353</b>	<b>2.2</b>	<b>0.00</b>	<b>11</b>	<b>W (*)</b>
Sihla-1	357	2	1.8	16	T–W
(Vepor Mts.)	<b>356.1</b>	<b>2</b>	<b>0.99</b>	<b>16</b>	<b>W (*)</b>
CH SK-1	357	3	1.9	8	T–W
(Čierna Hora Mts.)	<b>356.4</b>	<b>2.4</b>	<b>0.58</b>	<b>8</b>	<b>W (*)</b>

Therefore it precipitated from a relatively oxidizing and water enriched environment, exclusively in the granitic rocks with higher CaO/Al<sub>2</sub>O<sub>3</sub> (wt. %) bulk rock ratio (0.15–0.25) and ≥0.4 wt. % TiO<sub>2</sub> (Broska et al. 2004).

Variscan calc-alkaline granitic rocks of I- and S-type affinity belong to the most voluminous lithologies within Paleozoic crystalline basement of the West-Carpathian Tatric and Veporic units. Their age of magmatic crystallization has been determined recently by single-grain and in situ U–Pb dating of zircon and monazite. The dating ages are usually between ~360 and 340 Ma (Upper Devonian to Carboniferous); they indicate a main interval of Variscan plutonic activity in the West-Carpathian Tatric and Veporic crystalline basement (e.g., Poller et al. 2000; Gaab et al. 2005; Burda & Gawęda 2009; Kohút et al. 2009; Broska et al. 2013; Burda et al. 2013a, b; Gawęda et al. 2016). This age interval is also corroborated by chemical U–Th–Pb dating of monazite (e.g., Finger et al. 2003; Uher et al. 2014) and some older Rb–Sr whole-rock isochron data (Cambel et al. 1990 and references therein). Such Upper Devonian to early Carboniferous granitic magmatism belongs to older phase of plutonic activity, located within internal parts of the Variscan orogen for example in the Hintertal Plutonic Suite (mainly the Pletzen Pluton) of the Seckau Complex, Austroalpine basement of the Eastern Alps (Mandl et al. 2018), in part of the Moldanubian plutonic complex (Weinsberg granite) and the Central Bohemian Batholith (Sázava granodiorite; Cháb et al. 2008; Žák et al. 2014 and references therein), in southern Schwarzwald and NW part of the French Massif Central, e.g. Guéret batholith (Kroner & Romer 2013 and references therein).

Our SHRIMP U–Pb titanite results also reveal Variscan age interval between 351±6.5 and 338±6 Ma, which corresponds to early Carboniferous, Tournaisian to Viséan stage (Table 5, Fig. 7). However, they are systematically lower (~5 to 19 Ma) in comparison with zircon U–Pb ages of 353–356±2 Ma achieved by in-situ SIMS method from the same titanite-bearing granitic rocks from the Western Carpathians (Broska et al. 2013; Table 5).

Here we suggest the following two most plausible interpretations of this age discrepancy: (1) the titanite ages indicate their younger, late-magmatic crystallization in contrast to the early-magmatic age of zircon precipitation; or (2) post-magmatic (subsolidus) origin of titanite due to younger event connected with subsequent overprint of the parental granitic rocks (discussed below).

For estimating of titanite crystallization temperature [ $T_s(Ttn)$ ], we apply the Zr-in-titanite thermobarometry (Hayden et al. 2008). This geothermobarometer is dependent on Zr content in titanite as well as activity of coexisting quartz [ $a(SiO_2)$ ] and rutile [ $a(TiO_2)$ ] in the investigating rock, where  $a(SiO_2)=a(TiO_2)=1.0$  for quartz- and rutile-bearing rocks. However, rutile does not identify in our tonalites to granodiorites; instead of ilmenite, Ti-bearing magnetite, biotite and allanite-(Ce) represent principal carriers of Ti here. In such rutile-absent magmatic rocks,  $a(TiO_2)$  attains values ≥0.6 but most of the ilmenite- and biotite-bearing rocks are nearly rutile saturated (Hayden & Watson 2007; Ferry & Watson 2007; Chambers & Kohn 2012). We calculate  $a(TiO_2)=0.6$  to 1.0 for estimating of possible interval of  $T_s(Ttn)$ . The maximum  $T_s(Ttn)$  was achieved at  $a(TiO_2)=1.0$ ; the activity below 1.0 produced slightly decreasing of this temperature. For example, for  $a(TiO_2)=0.9$  and 0.6, the  $T_s(Ttn)$  were 5–6 °C and 24 to 28 °C lower, respectively (Table 6). Pressure represents the other important parameter, influencing the  $T_s(Ttn)$ . We apply pressures of 0.2 to 0.4 GPa as the most realistic values for magmatic emplacement, initial cooling and uplift of common orogen-related granitic intrusions. The emplacement/solidification pressure of the West-Carpathian titanite-bearing I-type granitic rocks, calculated based on Al-in-hornblende geobarometry attains ~0.35 to 0.4 GPa (Petrik & Broska 1994; Broska et al. 1997). The pressure (P) positively correlates with  $T_s(Ttn)$ ; the values are 22–24 °C higher at P=0.4 GPa with a comparison of 0.2 GPa, using the same  $a(TiO_2)$  value. Consequently, the Zr-in-titanite thermobarometry reveal  $T_s(Ttn)=650–750$  °C for  $a(TiO_2)=0.6–1.0$  and P=0.2–0.4 GPa for the investigated granitic rocks (Table 6).

Interpretation of such temperature is also dependent on the diffusion rate and corresponding Zr closure temperature in titanite [ $T_c(Zr(Ttn))$ ]. This parameter is further a function of titanite crystal size and cooling rate. Our titanite crystals are relatively large, ~0.5 to 10 mm across (Figs. 2–3, 6). Such large crystal size secured retention (negligible Zr diffusion) of titanite at the temperature ≥750 °C during 10<sup>7</sup>–10<sup>8</sup> years at common cooling rate of ~10–100 °C/Ma (Cherniak 2006; Hayden et al. 2008; Kirkland et al. 2016, 2018; Kohn 2017). However, the measured U–Pb ages are additionally influenced

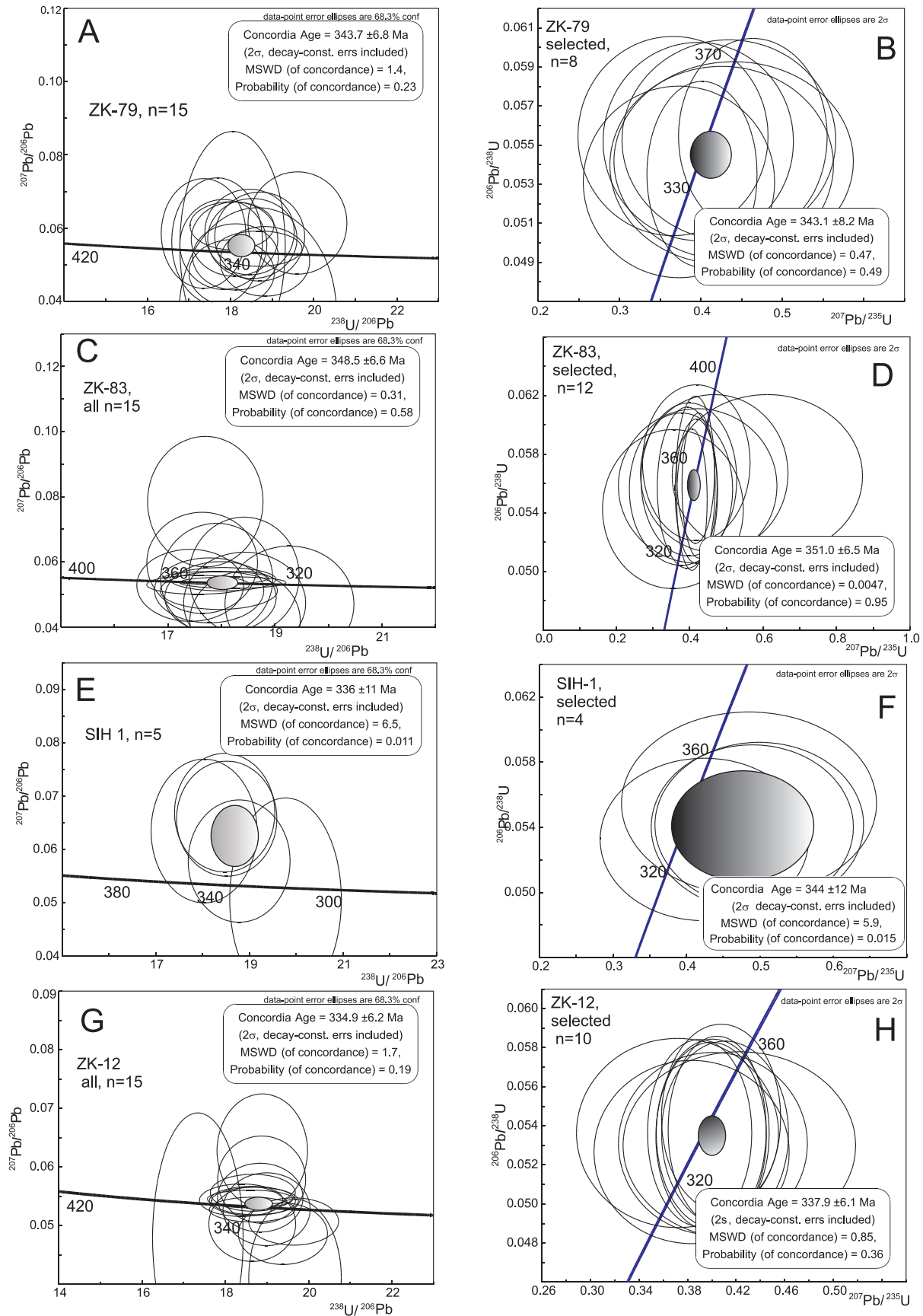


**Fig. 7.** The U–Pb concordia age diagrams of titanite from the West-Carpathian granitic rocks. Left column: Tera–Wasserburg diagrams of all spots; right column: Wetherill diagrams of selected spot analyses (see Table 4). All uncertainties are quoted at 2-sigma level.

by possible partial loss of Pb from titanite lattice expressed as Pb closing temperature in titanite [ $T_c\text{Pb(Ttn)}$ ]. The  $T_c\text{Pb(Ttn)}$  is generally lower than  $T_c\text{Zr(Ttn)}$ , due to the higher mobility of Pb with comparison to Zr (Cherniak 2006; Kirkland et al.

2016, 2018). Nevertheless,  $T_c\text{Pb(Ttn)}$  is also relatively high ( $\geq 700\text{--}800\text{ }^\circ\text{C}$ ) for large titanite crystals ( $\geq 0.5\text{ mm}$ ) at cooling rate of  $\sim 10\text{--}100\text{ }^\circ\text{C/Ma}$  (Gao et al. 2012; Sun et al. 2012; Spencer et al. 2013; Kohn 2017). Based on above calculations and assumptions, we can conclude  $T_c\text{Zr(Ttn)} > T_c\text{Pb(Ttn)} > T_s\text{(Ttn)}$  for our granitic rocks and therefore the calculated  $T_s\text{(Ttn)}$  are not influenced by Zr and Pb mobility in the studied titanite crystals. Consequently, our data represent rather true precipitation temperatures at the measured age than the age of titanite closure temperature.

If we consider the late-magmatic origin of titanite, a time of magmatic evolution, including pluton accretion and mineral crystallization from the solidified melt of the parental granite is necessary to take into consideration. Recent growing dataset of evidence suggests that granitic pluton emplacement and assembly occurs by incremental accretion of numerous successive and relatively small pulses of magma with little liquid that accumulates by dyke-like propagation over variable time periods, generally from  $10^2$  to  $10^6$  years, depending of geodynamic setting and source fertility (e.g., Coleman et al. 2004; Glazner et al. 2004; Michel et al. 2008; Schaltegger et al. 2009; Barboni et al. 2013). Sensitive in-situ zircon U–Pb geochronological data indicate amalgamation of large granitic batholiths ( $\sim 10^3$  to  $10^4\text{ km}^2$  in their maximum extent) during approximately 5 to 10 Ma, in contrast to emplacement time of smaller composite plutons ( $< 10^3\text{ km}^2$ ;  $\sim 1.5\text{ Ma}$ ), and especially to one distinct magmatic pulse or small single plutons which create only during  $10^4$  to  $10^5$  years (e.g., Matzel et al. 2006; Michel et al. 2008; Carichi et al. 2012). Complete amalgamation time of the West-Carpathian I-type granitic plutons ( $\sim 10^2$  to  $10^3\text{ km}^2$  in order of magnitude) could be estimated over  $\sim 10\text{ Ma}$ , including numerous magmatic pulses. The model of long-lasting incremental growing of granitic pluton formed by repeated magma injections into an active shear zone during over  $\sim 30\text{ Ma}$  period has been recently applied for Variscan composite polygenetic intrusion of the Tatra granitoid pluton (Gawęda et al. 2016). On the other hand, the age difference between zircon and titanite U–Pb ages for the same granitic rocks in our case ( $\sim 5$  to  $19\text{ Ma}$ ; Table 5) is generally too large. For example, the Re di Castello pluton in Adamello granite batholith, Italy represents comagmatic crystallization of zircon and titanite during one or several closely subsequent magmatic pulses, where U–Pb dating of

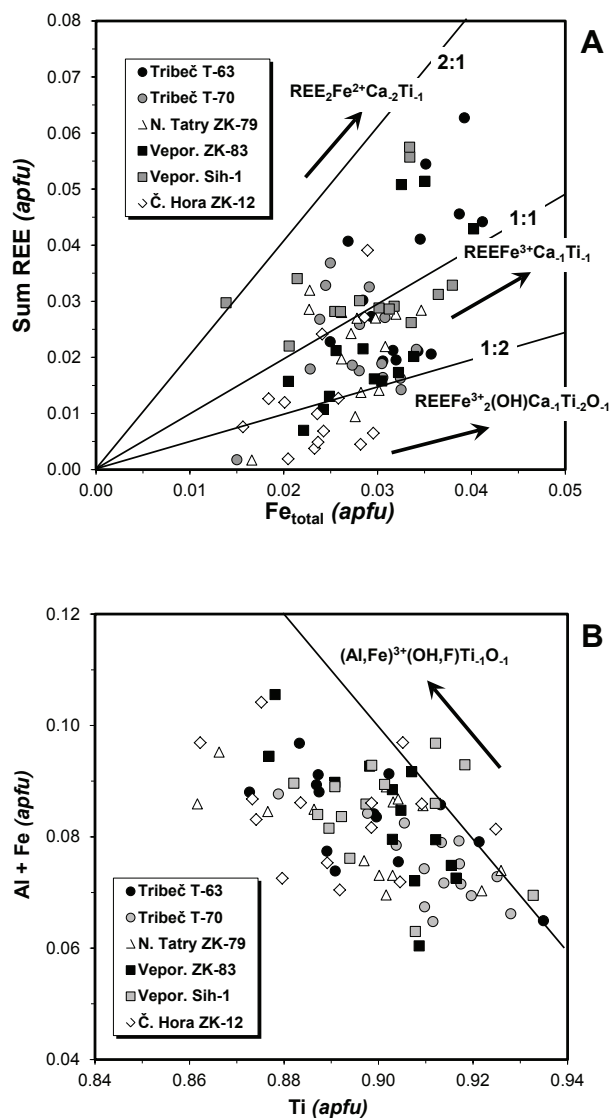


Fig. 8. Substitution diagrams and vectors of titanite from the West-Carpathian granitic rocks.

Table 6: Calculated titanite saturation temperature [ $T_s\text{(Ttn)}$ ] at various assumed pressure (0.2 to 0.4 GPa) based on average Zr concentration in titanite (Table 3) at  $a(\text{TiO}_2)=0.6$  and  $1.0$  (Hayden et al. 2008) and corresponding zircon saturation temperature [ $T_s\text{(Zrn)}$ ] (Watson & Harrison 1983).

Sample	Area	Zr (ppm)	$T_s\text{(Ttn)}$ ( $^\circ\text{C}$ ) at 0.2 GPa		$T_s\text{(Ttn)}$ ( $^\circ\text{C}$ ) at 0.3 GPa		$T_s\text{(Ttn)}$ ( $^\circ\text{C}$ ) at 0.4 GPa		$T_s\text{(Zrn)}$ ( $^\circ\text{C}$ )
			$a(\text{TiO}_2)$ 0.6	$a(\text{TiO}_2)$ 1.0	$a(\text{TiO}_2)$ 0.6	$a(\text{TiO}_2)$ 1.0	$a(\text{TiO}_2)$ 0.6	$a(\text{TiO}_2)$ 1.0	
T-63	Tribeč Mts.	406	698	726	710	738	722	750	797
T-70	Tribeč Mts.	285	680	707	692	718	703	730	
ZK-79	Nízke Tatry Mts.	234	671	696	682	708	693	720	779
ZK-83	Vepor Mts.	273	678	704	690	716	701	728	840
Sih-1	Vepor Mts.	357	692	719	703	731	715	743	808
ZK-12	Čierna Hora Mts.	155	651	675	662	687	673	698	829



titanite reveal only 130 to 700 ka younger ages than zircon (Schaltegger et al. 2009).

Textural patterns indicate titanite crystallization at the expense of magmatic Ti-rich magnetite, magnesian biotite and Ca-rich plagioclase which can be observed as armoured inclusions in titanite, where re-equilibration involved oxidation of the ulvöspinel ( $\text{Fe}^{2+}_2\text{TiO}_4$ ) component in Ti-rich magnetite produced titanite and Ti-poor magnetite in the Tribeč I-type granites (Broska et al. 2007). Titanite and epidote partly replace magmatic biotite and late-magmatic, Ti-poor magnetite is commonly overgrown by titanite in the Čierna Hora granitic rocks (Bónová et al. 2010). The calculation of a model mineral equilibrium in the  $\text{K}_2\text{O}-\text{CaO}-\text{FeO}-\text{Al}_2\text{O}_3-\text{TiO}_2-\text{SiO}_2-\text{H}_2\text{O}-\text{O}_2$  (KCFATSHO) system indicates that pure magnetite+titanite forms in granites as a product of the reaction between the early magmatic Ti-rich magnetite, Mg-rich biotite (phlogopite), and anorthite-rich plagioclase in a fluid-rich environment derived from a melt under relatively oxidizing conditions (Broska et al. 2007; Broska & Petřík 2011). The above-mentioned authors suggest a late-magmatic origin of titanite; assuming equilibrium among biotite, K-feldspar and magnetite, where the intersection of the calculated biotite stability curves with the curve of minimum water content in the haplogranite system (after Johannes & Holtz 1996) gives 4.8 wt.%  $\text{H}_2\text{O}$  at 744 °C and 0.4 GPa for the titanite-bearing tonalite of the Čierna Hora Mts. (Bónová et al. 2010). Application of the Fe–Ti oxide geothermometry (Sauerzapf et al. 2008; Ghiorsio & Evans 2008) show ~630 to 780 °C interval for the equilibrium of magnetite–ilmenite pair for the titanite-bearing granitic rocks (Tribeč, Čierna Hora; Broska & Petřík 2011). Moreover, this titanite producing reaction indicates the temperature of ~710 °C at 0.4 GPa pressure and  $a_{\text{H}_2\text{O}}=0.5$ , calculated using the Thermocalc 3.31 (Holland & Powell 2011) and the AX software for end-member activities (Broska & Petřík 2015). These calculated temperatures are in accordance with our results based on Zr-in-titanite thermometry (Table 6).

However, such temperatures (~650 to 750 °C) are near but mostly under tonalite solidus at ~0.3–0.4 GPa (e.g., Singh & Johannes 1996). Experiments indicate a beginning of dehydration melting in biotite–plagioclase–quartz assemblage of tonalite composition at 760 °C and 0.5 GPa, using biotite chemistry close to ~50 mol. % annite, 0.5 apfu Al and 0.3 apfu Ti in octahedral site (Singh & Johannes 1996) which is similar to the biotite composition of investigated West-Carpathian granitic rocks (Petřík 1980; Petřík & Broska 1989, 1994; Bónová et al. 2010).

After the formation of subduction-related I-type granites, subsequent Variscan crustal shortening during younger collisional event might have trigger partial melting and intrusion of limited amounts of leucogranitic melts and/or related high-temperature fluids into I-type tonalites to granodiorites, dated at ~340 Ma by chemical U–Th–Pb monazite method in the Tribeč Mts. (Broska & Petřík 2015) and Branisko near Čierna Hora (Bónová et al. 2005). Almandine garnet from granitic pegmatite near Rimavská Baňa (Veporic Unit) also reveals a Visean Sm–Nd isotopic age of  $339.0 \pm 7.7$  Ma (Thöni

et al. 2003). Another example of two magmatic pulses has been documented by LA–MC–ICP–MS U–Pb zircon dating from granitic rocks of the Tatry Mts., where the high luminescence zircon cores record age of  $350 \pm 3$  Ma, and younger, low luminescence zircon rims gives  $337 \pm 6$  Ma (Burda et al. 2013b).

Optical and BSE photomicrographs of the West-Carpathian granitic titanite and associated minerals (Broska et al. 2004, 2007; Broska & Petřík 2011, 2015) together with our results (Fig. 3) clearly document its complex evolution including growth and superimposed partial dissolution–reprecipitation and alteration phenomena. In some cases, primary titanite was partly to almost completely replaced by secondary ilmenite±epidote pseudomorphs with many pores (Broska et al. 2007). Complex textural patterns are characteristic feature of accessory titanite of various origin; they commonly occur in titanite crystals of volcanic (Nakada 1991; Colombini et al. 2011), plutonic (Paterson et al. 1989; Paterson & Stephens 1992; McLeod et al. 2011; Middleton et al. 2013) as well as post-magmatic and metamorphic origin (Černý et al. 1995; Cempírek et al. 2008). In our samples, we interpret such textures as a result of subsolidus, fluid-induced high-temperature precipitation of titanite during a Variscan post-magmatic event.

Moreover, the late irregular veinlets and irregular patchy zones of younger, secondary titanite occur along cleavage planes, fissures and crystal rims of primary titanite (Fig. 3G–H), commonly with secondary allanite-(Ce), epidote, quartz, albite, K-feldspar, chlorite, ilmenite,  $\text{TiO}_2$  phase (rutile and/or anatase), and hematite. This late mineral association could be connected with Alpine metamorphic overprint of the Variscan basement of the Western Carpathians, especially in the Veporic Unit, where Cretaceous (~100 to 70 Ma) metamorphic conditions of the Kráľova Hoľa Complex attained 430–530 °C and 550–850 MPa (Janák et al. 2001; Jeřábek et al. 2008).

## Summary

The study of large titanite crystals (~0.5 to 10 mm) from Variscan I-type granitic rocks of the Western Carpathians allows the following main conclusions:

- Titanite, as a characteristic accessory mineral of Variscan I-type granitic rocks, commonly shows complex compositional oscillatory, sector and convolute zonal textures, reflecting mainly variations in Ca and Ti versus Al, Fe, REE ( $\leq 4.8$  wt. %  $\text{REE}_2\text{O}_3$ ), and Nb ( $\leq 0.5$  wt. %  $\text{Nb}_2\text{O}_5$ ).
- Following principal substitutions controlling the crystal chemistry were detected in the studied titanite:  $\text{REE}^{3+} + \text{Fe}^{3+} = \text{Ca}^{2+} + \text{Ti}^{4+}$ ,  $2\text{REE}^{3+} + \text{Fe}^{2+} = 2\text{Ca}^{2+} + \text{Ti}^{4+}$ , and  $(\text{Al}, \text{Fe})^{3+} + (\text{OH}, \text{F})^- = \text{Ti}^{4+} + \text{O}^{2-}$ .
- Chondrite-normalized REE patterns of titanite show convex shapes from La to Sm, usually slightly negative Eu anomalies and almost regularly gradual decreasing of HREE's from Gd to Lu.
- U–Pb SHRIMP dating of titanite yield the Variscan ages of  $351.0 \pm 6.5$  to  $337.9 \pm 6.1$  Ma interval (Carboniferous, late

Tournaisian to Viséan). These ages are ~5 to 19 Ma younger than the primary magmatic U–Pb ages of zircon in corresponding rocks (Broska et al. 2013).

- Application of Zr-in-titanite geothermometry implies a possibly fluid-driven relatively high-temperature titanite precipitation, ~650 to 750 °C at inferred pressure of 0.2 to 0.4 GPa and  $a(\text{TiO}_2)=0.6\text{--}1.0$ .
- Mineral assemblage, U–Pb age dating and geothermometry indicate possible late-magmatic but rather early post-magmatic (subsidius) origin of investigated titanite. The post-magmatic precipitation of titanite was probably connected with a subsequent Variscan tectono-thermal event (~340±10 Ma), probably related with younger small granite intrusions and increased fluid activity.
- Veinlets and replacement zones of secondary titanite in the association of other late minerals (epidote, quartz, albite, K-feldspar, chlorite, ilmenite, rutile and/or anatase, and hematite) are probably products of Alpine (Cretaceous) metamorphic overprint.

**Acknowledgements:** This research was supported by the Slovak Research and Development Agency under contracts APVV-14-0278, APVV-15-0050, VEGA Agency Nos. 1/0257/13 and 1/0499/15. Analytical assistance with the SHRIMP IIe/MC calibration was provided by Zbigniew Czupyt. We are grateful to Daniel Dunkley for his assistance on the beginning analytical works on titanite and to Anna Pietranik for procurement of the Khan titanite reference material. We also thank Igor Petřík (handling editor), Jolanta Burda and Adam Pieczka (both reviewers) for their critical and constructive suggestions.

## References

- Ackerson M.R. 2011: Trace element partitioning between titanite and groundmass in silicic volcanic systems. *MSc. Thesis, University of North Carolina*, Chapel Hill, U.S.A., 1–69.
- Aleinikoff J.N., Wintsch R.P., Fanning C.M. & Dorais M.J. 2002: U–Pb geochronology of zircon and polygenetic titanite from the Glastonbury Complex, Connecticut, USA: an integrated SEM, EMPA, TIMS, and SHRIMP study. *Chem. Geol.* 188, 125–147.
- Barboni M., Schoene B., Ovtchanova M., Bussy F., Schaltegger U. & Gerdes A. 2013: Timing of incremental pluton construction and magmatic activity in a back-arc setting revealed by ID-TIMS U/Pb and Hf isotopes on complex zircon grains. *Chem. Geol.* 340, 76–83.
- Barrat J.A., Zanda B., Moynier F., Bollinger C., Liorzou C. & Bayon G. 2012: Geochemistry of CI chondrites: Major and trace elements, and Cu and Zn isotopes. *Geochim. Cosmochim. Acta* 83, 79–92.
- Bauer J.E. 2015: Complex zoning patterns and rare earth element variations across titanite crystals from the Half Dome Granodiorite, central Sierra Nevada, California. *MSc. Thesis, University of North Carolina*, Chapel Hill, 1–76.
- Bea F. 1996: Residence of REE, Y, Th and U in granites and crustal protoliths; implications for the chemistry of crustal melts. *J. Petrol.* 37, 521–552.
- Bernau R. & Franz G. 1987: Crystal chemistry and genesis of Nb-, V-, and Al-rich metamorphic titanite from Egypt and Greece. *Can. Mineral.* 25, 695–705.
- Bezák V., Jacko S., Janák M., Ledru P., Petřík I. & Vozárová A. 1997: Main Hercynian lithotectonic units of the Western Carpathians. In: Grečula P., Hovorka D. & Putiš M. (Eds.): Geological evolution of the Western Carpathians. *Mineralia Slovaca Monographs*, Bratislava, 261–268.
- Bezák V., Biely A., Elečko M., Konečný V., Mello J., Polák M. & Potfaj M. 2011: A new synthesis of the geological structure of Slovakia – the general geological map at 1:200000 scale. *Geol. Quarterly* 55, 1–8.
- Bielik M., Šefára J., Kováč M., Bezák V. & Plašienka D. 2004: The Western Carpathians – interaction of Hercynian and Alpine processes. *Tectonophysics* 393, 63–86.
- Bonamici C.E., Fanning C.M., Kozdon R., Fournelle J.H. & Walley J.W. 2015: Combined oxygen-isotope and U–Pb zoning studies of titanite: New criteria for age preservation. *Chem. Geol.* 398, 70–84.
- Bónová K., Jacko S., Broska I. & Siman P. 2005: Contribution to geochemistry and geochronology of leucogranites from Branisko Mts. *Miner. Slov.* 37, 349–350 (in Slovak).
- Bónová K., Broska I. & Petřík I. 2010: Biotite from Čierna Hora Mountains granitoids (Western Carpathians, Slovakia) and estimation of water contents in granitoid melts. *Geol. Carpath.* 61, 3–17.
- Bouch J.E., Hole M.J. & Trewin N.H. 1997: Rare earth and high strength element partitioning behaviour in diagenetically precipitated titanites. *Neues Jahrb. Mineral. Abh.* 172, 3–21.
- Broska I. & Petřík I. 2011: Accessory Fe–Ti oxides in the West-Carpathian I-type granitoids: witnesses of the granite mixing and late oxidation processes. *Mineral. Petrol.* 102, 87–97.
- Broska I. & Petřík I. 2015: Variscan thrusting in I- and S-type granitic rocks of the Tribeč Mountains, Western Carpathians (Slovakia): evidence from mineral compositions and monazite dating. *Geol. Carpath.* 66, 455–471.
- Broska I. & Uher P. 1988: Accessory minerals of granitoid rocks of Bojná and Hlohovec blocks, the Považský Inovec Mts. *Geol. Carpath.* 39, 505–520.
- Broska I. & Uher P., 2001: Whole-rock chemistry and genetic typology of the West-Carpathian Variscan granites. *Geol. Carpath.* 52, 79–90.
- Broska I., Petřík I. & Benko P. 1997: Petrology of the Malá Fatra granitoid rocks (Western Carpathians, Slovakia). *Geol. Carpath.* 48, 27–37.
- Broska I., Vdovcová K., Konečný P., Siman P. & Lipka J. 2004: Accessory titanite in the granitoids of the Western Carpathians: distribution and composition. *Miner. Slov.* 36, 237–246 (in Slovak).
- Broska I., Harlov D., Tropper P. & Siman P. 2007: Formation of magmatic titanite–ilmenite phase relations during granite alteration in the Tribeč Mountains, Western Carpathians, Slovakia. *Lithos* 95, 58–71.
- Broska I., Petřík I., Be'eri-Shlevin Y., Majka J. & Bezák V. 2013: Devonian/Mississippian I-type granitoids in the Western Carpathians: A subduction-related hybrid magmatism. *Lithos* 162–163, 27–36.
- Brugger J. & Gieré R. 1999: As, Sb, Be and Ce enrichment in minerals from a metamorphosed Fe–Mn deposit, Val Ferrera, Eastern Swiss Alps. *Can. Mineral.* 37, 37–52.
- Burda J. & Gawęda A. 2009: Shear-influenced partial melting in the Western Tatra metamorphic complex: Geochemistry and geochronology. *Lithos* 110, 373–385.
- Burda J., Gawęda A. & Klötzli U. 2013a: Geochronology and petrogenesis of granitoid rocks from the Goryczkova Unit, Tatra Mountains (Central Western Carpathians). *Geol. Carpath.* 64, 419–435.
- Burda J., Gawęda A. & Klötzli U. 2013b: U–Pb zircon age of the youngest magmatic activity in the High Tatra granites (Central Western Carpathians). *Geochronometria* 40, 134–144.

- Burger A.J., von Knorring O. & Clifford T.N. 1965: Mineralogical and radiometric studies of monazite and sphene occurrences in the Namib Desert, South-West Africa. *Mineral. Mag.* 35, 519–528.
- Cambel B., Král J. & Burchart J. 1990: Isotopic geochronology of the Western Carpathian crystalline complex with catalogue of data. *Veda*, Bratislava, 1–184 (in Slovak with English summary).
- Carichi L., Annen C., Rust A. & Blundy J. 2012: Insights into the mechanisms and timescales of pluton assembly from deformation patterns of mafic enclaves. *J. Geophys. Res.* 117, B11206, 1–18.
- Carswell D.A., Wilson R.N. & Zhai M. 1996: Ultra-high pressure aluminous titanite in carbonate-bearing eclogites at Shuanghe in Dabieshan, central China. *Mineral. Mag.* 60, 461–471.
- Castelli D. & Rubatto D. 2002: Stability of Al- and F-rich titanite in metacarbonate: petrologic and isotopic constraints from a poly-metamorphic eclogitic marble of the internal Sesia Zone (Western Alps). *Contrib. Mineral. Petrol.* 142, 627–639.
- Cempírek J., Houzar S. & Novák M. 2008: Complexly zoned niobian titanite from hedenbergite skarn at Písek, Czech Republic, constrained by substitutions  $\text{Al}(\text{Nb,Ta})\text{Ti}_2$ ,  $\text{Al}(\text{F,OH})(\text{TiO})_1$  and  $\text{SnTi}_1$ . *Mineral. Mag.* 72, 1293–1305.
- Černý P., Novák M. & Chapman R. 1995: The  $\text{Al}(\text{Nb,Ta})\text{Ti}_2$  substitution in titanite: the emergence of a new species? *Mineral. Petrol.* 52, 61–73.
- Cháb J., Breiter K., Fatka O., Hladil J., Kalvoda J., Šimůnek Z., Štorch P., Vašíček Z., Zajíc J. & Zapletal J. 2008: Short geology of the Bohemian Massif basement and their Carboniferous and Permian cover. *Czech Geological Survey Press*, Prague, 1–284 (in Czech).
- Chakhmouradian A.R. 2004: Crystal chemistry and paragenesis of compositionally unique (Al-, Fe-, Nb-, and Zr-rich) titanite from Afrikanda, Russia. *Am. Mineral.* 89, 1752–1762.
- Chakhmouradian A.R., Reguir E.P. & Mitchell R.H. 2003: Titanite in carbonatitic rocks: Genetic dualism and geochemical significance. *Period. Mineral.* 72, Special Issue 1, Eurocarb workshop Italy, 107–113.
- Chambers J.A. & Kohn M.J. 2012: Titanium in muscovite, biotite, and hornblende: Modelling, thermometry and rutile activities in metapelites and amphibolites. *Am. Mineral.* 97, 543–555.
- Chen Y.-X. & Zheng Y.-F. 2015: Extreme Nb/Ta fractionation in metamorphic titanite from ultrahigh-pressure metagranite. *Geochim. Cosmochim. Acta* 150, 53–73.
- Chen Y.-X., Zhou K., Zheng Y.-F., Gao X.-Y. & Yang Y.-H. 2016: Polygenetic titanite records the composition of metamorphic fluids during the exhumation of ultrahigh-pressure metagranite in the Sulu orogen. *J. Metamorph. Geol.* 34, 573–594.
- Cherniak D.J. 2006: Zr diffusion in titanite. *Contrib. Mineral. Petrol.* 152, 639–647.
- Chew D.M., Petrus J.A. & Kamber B.S. 2014: U–Pb LA–ICP–MS dating using accessory mineral standards with variable common Pb. *Chem. Geol.* 363, 185–199.
- Coleman D.S., Gray W. & Glazner A.F. 2004: Rethinking the emplacement and evolution of zoned plutons: geochronologic evidence for incremental assembly of the Tuolumne Intrusive Suite, California. *Geology* 32, 433–436.
- Colombini L.L., Miller C.F., Gualda G.A.R., Wooden J.L. & Miller J.S. 2011: Sphene and zircon in the Highland Range volcanic sequence (Miocene, southern Nevada, USA): elemental partitioning, phase relations, and influence on evolution of silicic magma. *Mineral. Petrol.* 102, 29–50.
- Della Ventura G. & Bellatreccia F. 1999: Zr- and LREE-rich titanite from Tre Croci, Vico Volcanic complex (Latium, Italy). *Mineral. Mag.* 63, 123–130.
- Ferry J.M. & Watson E.B. 2007: New thermodynamic models and revised calibrations for the Ti-in-zircon and Zr-in-rutile thermometers. *Contrib. Mineral. Petrol.* 154, 429–437.
- Finger F., Broska I., Haunschmidt B., Hraško L., Kohút M., Krenn E., Petrik I., Riegler G. & Uher P. 2003: Electron-microprobe dating of monazites from Western Carpathian basement granitoids: plutonic evidence for an important Permian rifting event subsequent to Variscan crustal anatexis. *Int. J. Earth Sci.* 92, 86–98.
- Foord E.E., Hlava P.F., Erd R.C. & Lichte F.E. 1993: Rhyolite-hosted REE–Fe–Nb-bearing titanite from Willow Spring Draw, Sierra County, New Mexico, U.S.A. In: Rare earth minerals: chemistry, origin and ore deposits. 1 and 2 April 1993. Abstracts. *The Natural History Museum London*, United Kingdom, 39–41.
- Gaob A.S., Poller U., Janák M., Kohút M. & Todt W. 2005: Zircon U–Pb geochronology and isotopic characterization for the pre-Mesozoic basement of the Northern Veporic Unit (Central Western Carpathians, Slovakia). *Schweiz. Mineral. Petrogr. Mitt.* 85, 69–88.
- Gao X.-Y., Zheng Y.-F. & Chen Y.-X. 2011: U–Pb ages and trace elements in metamorphic zircon and titanite from UHP eclogite in the Dabie orogen: constraints on P–T–t path. *J. Metamorph. Geol.* 29, 721–740.
- Gao X.-Y., Zheng Y.-F., Chen Y.-X. & Guo J. 2012: Geochemical and U–Pb age constraints on the occurrence of polygenetic titanites in UHP metagranite in the Dabie orogen. *Lithos* 136–139, 93–108.
- Gasser D., Jeřábek P., Faber C., Stünitz, H., Menegon L., Corfu F., Erambert M. & Whitehouse M.J. 2015: Behaviour of geochronometers and timing of metamorphic reactions during deformation at lower crustal conditions: phase equilibrium modeling and U–Pb dating of zircon, monazite, rutile and titanite from the Kalak Nappe Complex, northern Norway. *J. Metamorph. Geol.* 33, 513–534.
- Gawęda A., Burda J., Klötzli U., Golonka J. & Szopa K. 2016: Episodic construction of the Tatra granitoid intrusion (Central Western Carpathians, Poland/Slovakia): consequences for the geodynamics of Variscan collision and Rheic Ocean closure. *Int. J. Earth Sci.* 105, 1153–1174.
- Ghiorso M.S. & Evans B.W. 2008: Thermodynamics of rhombohedral oxide solid solutions and a revision of the Fe–Ti two-oxide geothermometer and oxygen-barometer. *Am. J. Sci.* 308, 957–1039.
- Gieré R. 1992: Compositional variation of metasomatic titanite from Adamello (Italy). *Schweiz. Mineral. Petrogr. Mitt.* 72, 167–177.
- Glazner A.F., Bartley J.M., Coleman D.S., Gray W. & Taylor R.Z. 2004: Are plutons assembled over millions of years by amalgamation from small magma chambers? *GSA Today* 14, 4–11.
- Green T.H. & Pearson N.J. 1986: Rare-earth element partitioning between sphene and coexisting silicate liquid at high pressure and temperature. *Chem. Geol.* 55, 105–119.
- Gromet L.P. & Silver L.T. 1983: Rare earth element distribution among minerals in a granodiorite and their petrogenetic implications. *Geochim. Cosmochim. Acta* 47, 925–939.
- Hayden L.A., Watson E.B. & Wark D.A. 2008: A thermometer for sphene (titanite). *Contrib. Mineral. Petrol.* 155, 529–540.
- Heaman L.M. 2009: The application of U–Pb geochronology to mafic, ultramafic and alkaline rocks: an evolution of the three mineral standards. *Chem. Geol.* 261, 43–52.
- Higgins J.B. & Ribbe P.H. 1976: The crystal chemistry and space groups of natural and synthetic titanites. *Am. Mineral.* 61, 878–888.
- Holland T.J.B. & Powell R. 2011: An improved and extended internally consistent thermodynamic dataset for phases of petrological interest, involving a new equation of state for solids. *J. Metamorph. Geol.* 29, 333–383.
- Hoskin P.W.O., Kinny P.D., Wyborn D. & Chappell B.W. 2000: Identifying accessory mineral saturation during differentiation in granitoid magmas: an integrated approach. *J. Petrol.* 41, 1365–1396.

- Hovorka D. 1960: Contribution to petrography of Veporide granitoids. *Acta Geol. Geogr. Univ. Comen. Geol.* 4, 255–262 (in Slovak).
- Hovorka D. & Hvožd'ara P. 1964: Accessory minerals of the Veporide granitoid rocks. *Acta Geol. Geogr. Univ. Comen. Geol.* 9, 145–179 (in Slovak).
- Jacko S. & Petrík I. 1987: Petrology of the Čierna hora Mts. granitoid rocks. *Geol. Carpath.* 38, 515–544.
- Janák M., Plašienka D., Frey M., Cosca M., Schmidt S.Th., Lupták B. & Méres Š. 2001: Cretaceous evolution of a metamorphic core complex, the Veporic unit, Western Carpathians (Slovakia): P–T conditions and in situ  $^{40}\text{Ar}/^{39}\text{Ar}$  UV laser probe dating of metapelites. *J. Metamorph. Geol.* 19, 197–216.
- Jeřábek P., Janák M., Faryad S.W., Finger F. & Konečný P. 2008: Polymetamorphic evolution of pelitic schists and evidence for Permian low-pressure metamorphism in the Vepor Unit, West Carpathians. *J. Metamorph. Geol.* 26, 465–485.
- Johannes W. & Holtz F. 1996: Petrogenesis and experimental petrology of granitic rocks. *Springer*, Berlin – Heidelberg – New York, 1–335.
- Kennedy A.K., Kamo S.L., Nasdala L. & Timms N.E. 2010: Grenville skarn titanite: potential reference material for SIMS U–Th–Pb analysis. *Can. Mineral.* 48, 1423–1443.
- Kinny P.D., McNaughton N.J., Fanning C.M. & Maas R. 1994: 518 Ma sphene (titanite) from the Khan pegmatite, Namibia, southwest Africa: a potential ion-microprobe standard. Abstract, 8th International Conference on Geochronology, Cosmochronology and Isotope Geology. *U.S. Geological Survey*, 171. Circular 1107.
- Kirkland C.L., Spaggiari C.V., Johnson T.E., Smithies R.H., Danišik M., Evans N., Wintage M.T.D., Clark C., Spencer C., Mikucki E. & McDonald B.J. 2016: Grain size matters: Implications for element and isotopic mobility in titanite. *Precambrian Res.* 278, 283–302.
- Kirkland C.L., Hollis J., Danišik M., Petersen J., Evans N.J. & McDonald B.J. 2018: Apatite and titanite from the Karrat Group, Greenland; implications for charting the thermal evolution of crust from the U–Pb geochronology of common Pb bearing phases. *Precambrian Res.* 300, 107–120.
- Knoche R., Angel R.J., Seifert F. & Fliervoet T.F. 1998: Complete substitution of Si for Ti in titanite  $\text{Ca}(\text{Ti}_{1-x}\text{Si}_x)\text{V}_2\text{Si}^{\text{IV}}\text{O}_5$ . *Am. Mineral.* 83, 1168–1175.
- Kohn M.J. 2017: Titanite petrochronology. *Rev. Mineral. Geochem.* 83, 419–441.
- Kohn M.J. & Corrie S.L. 2011: Preserved Zr-temperatures and U–Pb ages of high-grade metamorphic titanite: Evidence for a static hot channel in the Himalayan orogen. *Earth. Planet. Sci. Lett.* 311, 136–143.
- Kohút M. & Nabelek P.I. 2008: Geochemical and isotopic (Sr, Nd and O) constraints on sources of Variscan granites in the Western Carpathians. *J. Geosci.* 53, 307–322.
- Kohút M., Kovach V.P., Kotov A.B., Salnikova E.B. & Savatenkov V.M. 1999: Sr and Nd isotope geochemistry of Variscan granitic rocks from the Western Carpathians – implications for granite genesis and crustal evolution. *Geol. Carpath.* 50, 477–487.
- Kohút M., Uher P., Putiš M., Ondrejka M., Sergeev S., Larionov N. & Paderin I. 2009: SHRIMP U–Th–Pb zircon dating of the granitoid massifs in the Malé Karpaty Mountains (Western Carpathians): evidence of Meso-Variscan successive S- to I-type granitic magmatism. *Geol. Carpath.* 60, 345–350.
- Kowallis B.J., Christiansen E.H. & Griffen D.T. 1997: Compositional variations in titanite. *Geological Society of America Abstracts with Programs* 29, A-402.
- Kowallis B.J., Christiansen E.H., Dorais M., Winkel A., Henze P., Franzen L. & Webb H. 2018: Compositional variations of Fe, Al, and F in titanite (sphene). *Geological Society of America Annual Meeting, Indianapolis, Indiana, USA, 2018*, Paper No. 137-11.
- Kroner U. & Romer R.L. 2013: Two plates – many subduction zones: the Variscan orogeny reconsidered. *Gondwana Res.* 24, 298–329.
- Li J.-W., Deng X.-D., Zhou M.F., Liu Y.-S., Zhao X.-F. & Guo J.-L. 2010: Laser ablation ICP-MS titanite U–Th–Pb dating of hydrothermal ore deposits: A case study of the Tonglushan Cu–Fe–Au skarn deposit, SE Hubei Province, China. *Chem. Geol.* 270, 56–67.
- Liferovich R.P. & Mitchell R.H. 2005: Solid solution of rare earth elements in synthetic titanite: a reconnaissance study. *Mineral. Petrol.* 83, 271–282.
- Liferovich R.P. & Mitchell R.H. 2006: Solid solutions of niobium in synthetic titanite. *Can. Mineral.* 44, 1089–1097.
- Liu Y., Fan Y., Zhou T., Zhang L., Noel C., White N.C., Hong H. & Zhang W. 2018: LA-ICP-MS titanite U–Pb dating and mineral chemistry of the Luohe magnetite-apatite (MA)-type deposit in the Lu-Zong volcanic basin, Eastern China. *Ore Geol. Rev.* 92, 284–296.
- Ludwig K.R. 2003: User's Manual for Isoplot 3.00: A Geochronological toolkit for Microsoft Excel. *Berkeley Geochron. Center Spec. Publ.* 4, Berkeley, 1–70.
- Ludwig K.R. 2009: SQUID 2: A User's Manual, rev.12 April 2009. *Berkeley Geochronology Center Special Publication* 5, 1–110.
- Lyakhovich V.V. 1968: Accessory minerals. *Nauka*, Moscow, 1–276 (in Russian).
- Ma Q., Evans N.J., Ling X.-X., Yang J.-H., Wu F.-W., Zhao Z.-D. & Yang Y.-H. 2019: Natural Titanite reference materials for in situ U–Pb and Sm–Nd isotopic measurements by LA–(MC)–ICP–MS. *Geostand. Geoanal. Res.* 43, 355–384.
- Mandl M., Kurz W., Hauzenberger C., Fritz H., Klötzli U. & Schuster R. 2018: Pre-Alpine evolution of the Seckau Complex (Austroalpine basement/Eastern Alps): Constraints from in-situ LA-ICP-MS U–Pb zircon geochronology. *Lithos* 296–299, 412–430.
- Markl G. & Piazzolo S. 1999: Stability of high-Al titanite from low-pressure calcisilicates in light of fluid and host-rock composition. *Am. Mineral.* 84, 37–47.
- Matzel J.E.P., Bowring S.A. & Miller R.B. 2006: Time scales of pluton construction at differing crustal levels: Examples from the Mount Stuart and Tenpeak intrusions, North Cascades, Washington. *Geol. Soc. Am. Bull.* 118, 1412–1430.
- McLeod G.W., Dempster T.J. & Faithfull J.W. 2011: Deciphering magma-mixing processes using zoned titanite from the Ross of Mull Granite, Scotland. *J. Petrol.* 52, 55–82.
- Michel J., Baumgartner L., Putlitz B., Schaltegger U. & Ovtcharova M. 2008: Incremental growth of the Patagonian Torres del Paine laccolith over 90 k.y. *Geology* 36, 459–562.
- Middleton A.W., Förster H.-J., Uysal I.T., Golding S.D. & Rhede D. 2013: Accessory phases from the Soultz monzogranite, Soultz-sous-Forêts, France: Implications for titanite destabilisation and differential REE, Y and Th mobility in hydrothermal systems. *Chem. Geol.* 335, 105–117.
- Nakada S. 1991: Magmatic processes in titanite-bearing dacites, central Andes of Chile and Bolivia. *Am. Mineral.* 76, 548–560.
- Paterson B.A. & Stephens W.E. 1992: Kinetically induced compositional zoning in titanite: implications for accessory-phase/melt partitioning of trace elements. *Contrib. Mineral. Petrol.* 109, 373–385.
- Paterson B.A., Stephens W.E. & Herd D.A. 1989: Zoning in granitoid accessory minerals as revealed by backscattered electron imagery. *Mineral. Mag.* 53, 55–61.
- Paul B.J., Černý P., Chapman R. & Hinthorne J.R. 1981: Niobian titanite from the Huron Claim pegmatite, Southeastern Manitoba. *Can. Mineral.* 19, 549–552.

- Perseil E.-A. & Smith D.C. 1995: Sb-rich titanite in the manganese concentrations at St. Marcel-Praborna, Aosta Valley, Italy: petrography and crystal-chemistry. *Mineral. Mag.* 59, 717–734.
- Petrík I. 1980: Biotites from granitoid rocks of the West Carpathians and their petrogenetic importance. *Geol. Carpath.* 31, 215–230.
- Petrík I. & Broska I. 1989: Mafic enclaves in granitoid rocks of the Tribeč Mts., Western Carpathians: geochemistry and petrology. *Geol. Carpath.* 40, 667–696.
- Petrík I. & Broska I. 1994: Petrology of two granite types from the Tribeč Mountains, Western Carpathians: an example of allanite (+magnetite) versus monazite dichotomy. *Geol. J.* 29, 59–78.
- Petrík I. & Kohút M. 1997: The evolution of granitoid magmatism during the Variscan orogen in the Western Carpathians. In: Grecula P., Hovorka D., Putiš M. (Eds.): Geological evolution of the Western Carpathians. *Miner. Slov., Monograph*, 235–252.
- Pieczka A., Hawthorne F.C., Ma C., Rossman G.R., Szeleg E., Szuskiewicz A., Turniak K., Nejbort K., Ilnicki S.S., Buffat P. & Rutkowski B. 2017: Zabińskiite, ideally  $\text{Ca}(\text{Al}_{0.5}\text{Ta}_{0.5})(\text{SiO}_4)\text{O}$ , a new mineral of the titanite group from the Piława Górna pegmatite, the Góry Sowie Block, southwestern Poland. *Mineral. Mag.* 81, 591–610.
- Poller U., Janák M., Kohút M. & Todt W. 2000: Early Variscan magmatism in the Western Carpathians: U–Pb zircon data from granitoids and orthogneisses of the Tatra Mountains (Slovakia). *Int. J. Earth Sci.* 89, 336–349.
- Poller U., Todt W., Kohút M. & Janák M. 2001: Nd, Sr, Pb isotope study of the Western Carpathians: implication for Palaeozoic evolution. *Schweiz. Mineral. Petrogr. Mitt.* 81, 159–174.
- Putiš M. 1992: Variscan and Alpidic nappe structures of the Western Carpathian crystalline basement. *Geol. Carpath.* 43, 369–380.
- Radziszewski P. 1924: About the Carpathian granites. *Prace Polsk. Inst. Geol.* 1 (1921–1924), 97–154 (in Polish with French summary).
- Resor P.G., Chamberlain K.R., Frost C.D., Snoko A.W. & Frost B.R. 1996: Direct dating of deformation: U–Pb age of syndeformational sphene growth in the Proterozoic Laramie Peak shear zone. *Geology* 24, 623–626.
- Ribbe P.H. 1980: Titanite. In: Ribbe P.H. (Ed.): Orthosilicates. *Rev. Mineral.* 5, 137–154.
- Rubatto D. & Hermann J. 2001: Exhumation as fast as subduction? *Geology* 29, 3–6.
- Russell J.K., Groat L.A. & Halleran A.A.D. 1994: LREE-rich niobian titanite from Mount Bisson, British Columbia: Chemistry and exchange mechanisms. *Can. Mineral.* 32, 575–587.
- Sato K., Siga O.Jr., Basel M.A.S., Tassinari C.C.G. & Onoe A.T. 2016: SHRIMP U–Th–Pb analyses of titanites: analytical techniques and examples of terranes of the South-Southeast of Brazil – Geoscience Institute of the University of São Paulo. *Geol. Sér. Cient. Univ. São Paulo* 16, 3–18.
- Sauerzapf U., Lattard D., Burchard M. & Engelmann R. 2008: The titanomagnetite–ilmenite equilibrium: new experimental data and thermooxybarometric application to the crystallization of basic to intermediate rocks. *J. Petrol.* 49, 1161–1185.
- Schafarzik F. 1898: Industrial rocks of the Nitra Comitatus. *Földt. Kozl.* 28, 369–399 (in Hungarian).
- Schaltegger U., Brack P., Ovtcharova M., Peytcheva I., Schoene B., Stracke A., Marocchi M. & Bargossi G.M. 2009: Zircon and titanite recording 1.5 million years of magma accretion, crystallization and initial cooling in a composite pluton (southern Adamello batholith, northern Italy). *Earth Planet. Sci. Lett.* 286, 208–218.
- Simonetti A., Heaman L.M., Chacko T. & Banerjee N.R. 2006: In situ petrographic thin section U–Pb dating of zircon, monazite, and titanite using laser ablation–MC–ICP–MS. *Int. J. Mass Spectr.* 253, 87–97.
- Singh J. & Johannes W. 1996: Dehydration melting of tonalites. Part I. Beginning of melting. *Contrib. Mineral. Petrol.* 125, 16–25.
- Skublov S.G., Berezin A.V., Rizvanova N.G., Meľnik A.E. & Myskova T.A. 2014: Multistage Svecofennian metamorphism: Evidence from the composition and U–Pb age of titanite from eclogites of the Belomorian mobile belt. *Petrology* 22, 381–388.
- Speer J.A. & Gibbs G.V. 1976: The crystal structure of synthetic titanite,  $\text{CaTiOSiO}_4$ , and the domain textures of natural titanites. *Am. Mineral.* 61, 238–247.
- Spencer K.J., Hacker B.R., Kylander-Clark A.R.C., Andersen T.B., Cottle J.M., Stearns M.A., Poletti J.E. & Seward G.G.E. 2013: Campaign-style titanite U–Pb dating by laser-ablation ICP: Implications for crustal flow, phase transformations and titanite closure. *Chem. Geol.* 341, 84–101.
- Stacey J.S. & Kramers J.D. 1975: Approximation of terrestrial lead isotope evolution by a two-stage model. *Earth Planet. Sci. Lett.* 26, 207–221.
- Stearns M.A., Hacker B.R., Ratschbacher L., Rutte D. & Kylander-Clark A.R.C. 2015: Titanite petrochronology of the Pamir gneiss domes: Implications for middle to deep crust exhumation and titanite closure to Pb and Zr diffusion. *Tectonics* 34, 784–802.
- Stepanov A.V., Bekenova G.K., Levin V.L. & Hawthorne F.C. 2012: Natrotitanite, ideally  $(\text{Na}_{0.5}\text{Y}_{0.5})\text{Ti}(\text{SiO}_4)\text{O}$ , a new mineral from the Verkhnee Espe deposit, Akjilyautas Mountains, Eastern Kazakhstan district, Kazakhstan: description and crystal structure. *Mineral. Mag.* 76, 37–44.
- Sun J.F., Yang J.H., Wu F.Y., Xie L.W., Yang Y.H., Liu Z.C. & Li X.H. 2012: In situ U–Pb dating of titanite by LA-ICPMS. *Chin. Sci. Bull.* 57, 2506–2516.
- Thöni M., Petrík I., Janák M. & Lupták B. 2003: Preservation of Variscan garnet in Alpine metamorphosed pegmatite from the Veporic Unit, Western Carpathians: Evidence from Sm–Nd isotope data. *J. Czech Geol. Soc.* 48, 123–124.
- Tilton G.R. & Grünfelder M.C. 1968: Sphene: Uranium-lead ages. *Science* 159, 1458–1461.
- Uher P. & Broska I. 1995: Pegmatites in two suites of Variscan orogenic rocks (Western Carpathians, Slovakia). *Mineral. Petrol.* 55, 27–36.
- Uher P. & Broska I. 1996: Post-orogenic Permian granitic rocks in the Western Carpathian-Pannonian area: Geochemistry, mineralogy and evolution. *Geol. Carpath.* 47, 311–321.
- Uher P., Černý P., Chapman R., Határ J. & Miko O. 1998: Evolution of Nb-Ta minerals in the Prašivá granitic pegmatites, Slovakia: II. External hydrothermal Pb, Sb overprint. *Can. Mineral.* 36, 535–545.
- Uher P., Kohút M., Ondrejka M., Konečný P. & Šiman P. 2014: Monazite-(Ce) in Hercynian granites and pegmatites of the Bratislava Massif, Western Carpathians: Compositional variations and Th–U–Pb electron-microprobe dating. *Acta Geol. Slov.* 6, 215–231.
- Vlasov K.A., Sindeyeva N.D., Serdyuchenko D.P., Eshkova Je. M., Kuzmenko M.V. & Pyatenko Ju.A. 1964: Geochemistry, mineralogy and genetic types of rare-element deposits. Part II. Mineralogy of rare elements. *Nauka*, Moscow, 1–832 (in Russian).
- Vuorinen J.H. & Hälenius U. 2005: Nb-, Zr- and REE-rich titanite from the Alnö alkaline complex: Crystal chemistry and its importance as a petrogenetic indicator. *Lithos* 83, 128–142.
- Watson E.B. & Harrison T.M. 1983: Zircon saturation revisited: temperature and composition effects in a variety of crustal magma types. *Earth Planet. Sci. Lett.* 64, 295–304.
- Wones D.R. 1989: Significance of the assemblage titanite+magnetite+quartz in granitic rocks. *Am. Mineral.* 74, 744–749.

- Xie L., Wang R.-C., Chen J. & Zhu J.-C. 2010: Mineralogical evidence for magmatic and hydrothermal processes in the Qitianling oxidized tin-bearing granite (Hunan, South China): EMP and (MC)-LA-ICPMS investigations of three types of titanite. *Chem. Geol.* 276, 53–68.
- Zabavnikova N.I. 1957: Isomorphic substitutions in sphene. *Geochemistry* 3, 271–278 (in Russian).
- Žák J., Verner K., Janoušek V., Holub F.V., Kachlík V., Finger F., Hajná J., Tomek F., Vondrovic L. & Trubač J. 2014: A plate-tectonic model for the assembly of the Bohemian Massif constrained by structural relationships around granitoid plutons. In: Schulmann K., Martínez Catalán J.R., Lardeaux J.M., Janoušek V. & Oggiano G. (Eds.): *The Variscan Orogeny: Extent, timescale and the formation of the European crust. Geol. Soc. London, Spec. Publ.* 405, 169–196.
- Zoubek V. 1936: Notes about the crystalline basement of the Western Carpathians. *Věst. Stát. Geol. Úst. Českoslov. Rep.* 12, 207–239 (in Czech with German summary).

## Appendix

### *Titanite sample location:*

- T-63:** Biotite tonalite containing mafic magmatic enclaves. Zlatno village, Javorový Hill, a cliff 700 m S of the hilltop. Tribeč Mts. (48°29'20" N, 18°18'33" E).
- T-70:** Biotite tonalite, abandoned quarry, Nitra town, southern slope of Zobor Hill, Tribeč Mts. (48°19'38" N, 18°05'40" E).
- ZK-79:** Biotite granodiorite, Brusno village, confluence of Sopotnica and Studenec brooks, Nízke Tatry Mts. (48°51'59" N, 19°20'48" E).
- ZK-83:** Biotite tonalite, Hriňová village, outcrops on northern side of the dam, Vepor (Slovenské Rudohorie) Mts. (48°36'15" N, 19°32'41" E).
- Sih-1:** Biotite tonalite, Sihla village, Tlstý Javor quarry, Vepor (Slovenské Rudohorie) Mts. (48°41'04" N, 19°38'40" E).
- ZK-12:** Biotite tonalite, outcrop in road cut, Kysak village, Čierna Hora Mts. (48°52'08" N, 21°10'59" E).